




Article

RNA-seq and ChIP-seq Identification of Unique and Overlapping Targets of GLI Transcription Factors in Melanoma Cell Lines

Matea Kurtović¹, Nikolina Piteša¹, Nenad Bartoniček^{2,3}, Petar Ozretić¹ , Vesna Musani¹ , Josipa Čonkaš¹, Tina Petrić¹, Cecile King⁴ and Maja Sabol^{1,*} 

¹ Division of Molecular Medicine, Ruđer Bošković Institute, 10 000 Zagreb, Croatia

² The Garvan Institute of Medical Research, 384 Victoria St., Darlinghurst, NSW 2010, Australia

³ The Kinghorn Centre for Clinical Genomics, 370 Victoria St., Darlinghurst, NSW 2010, Australia

⁴ School of Biotechnology and Biomolecular Sciences, Faculty of Science, University of New South Wales, Sydney, NSW 2052, Australia

* Correspondence: maja.sabol@irb.hr



Citation: Kurtović, M.; Piteša, N.; Bartoniček, N.; Ozretić, P.; Musani, V.; Čonkaš, J.; Petrić, T.; King, C.; Sabol, M. RNA-seq and ChIP-seq Identification of Unique and Overlapping Targets of GLI Transcription Factors in Melanoma Cell Lines. *Cancers* **2022**, *14*, 4540. <https://doi.org/10.3390/cancers14184540>

Academic Editor: Mary J.C. Hendrix

Received: 11 August 2022

Accepted: 14 September 2022

Published: 19 September 2022

Publisher's Note: MDPI stays neutral with regard to jurisdictional claims in published maps and institutional affiliations.



Copyright: © 2022 by the authors. Licensee MDPI, Basel, Switzerland. This article is an open access article distributed under the terms and conditions of the Creative Commons Attribution (CC BY) license (<https://creativecommons.org/licenses/by/4.0/>).

Simple Summary: The majority of melanomas show hyperactivation of the MAPK signaling pathway, most often through mutations in *BRAF* and *NRAS*. Despite significant progress in therapy, targeting this signaling pathway solely has not been the solution for stopping the progression of this disease. Recently, researchers recognized the involvement of the Hedgehog-GLI (HH-GLI) signaling pathway in melanoma and its crosstalk with the MAPK pathway. In order to identify new HH-GLI-regulated targets that could be involved in the crosstalk with the MAPK pathway, we performed RNA sequencing and ChIP sequencing on three melanoma cell lines. By combining RNA-seq and ChIP-seq results, we successfully validated 15 novel targets of GLI proteins in melanoma cell lines. These findings will contribute to a better understanding of the GLI code and its role in melanoma.

Abstract: Background: Despite significant progress in therapy, melanoma still has a rising incidence worldwide, and novel treatment strategies are needed. Recently, researchers have recognized the involvement of the Hedgehog-GLI (HH-GLI) signaling pathway in melanoma and its consistent crosstalk with the MAPK pathway. In order to further investigate the link between the two pathways and to find new target genes that could be considered for combination therapy, we set out to find transcriptional targets of all three GLI proteins in melanoma. Methods: We performed RNA sequencing on three melanoma cell lines (CHL-1, A375, and MEL224) with overexpressed GLI1, GLI2, and GLI3 and combined them with the results of ChIP-sequencing on endogenous GLI1, GLI2, and GLI3 proteins. After combining these results, 21 targets were selected for validation by qPCR. Results: RNA-seq revealed a total of 808 differentially expressed genes (DEGs) for GLI1, 941 DEGs for GLI2, and 58 DEGs for GLI3. ChIP-seq identified 527 genes that contained GLI1 binding sites in their promoters, 1103 for GLI2 and 553 for GLI3. A total of 15 of these targets were validated in the tested cell lines, 6 of which were detected by both RNA-seq and ChIP-seq. Conclusions: Our study provides insight into the unique and overlapping transcriptional output of the GLI proteins in melanoma. We suggest that our findings could provide new potential targets to consider while designing melanoma-targeted therapy.

Keywords: melanoma; HH-GLI pathway; GLI targets; MAPK pathway; targeted therapy

1. Introduction

Melanoma is known as the most aggressive and deadliest of all skin cancers. The most often dysregulated signaling pathway in melanoma is RAS/RAF/MEK1/2-ERK1/2 (MAPK pathway). Almost 50% of all melanomas have a mutation in the *BRAF* gene, while 15–20% have a mutation in the *NRAS* gene [1], which leads to constitutive pathway

activation [2]. Still, targeting this signaling pathway solely has not been the solution for stopping the progression of this disease. Due to the low response rates of melanoma patients to targeted therapy and immunotherapy, novel treatment strategies are needed. Recently, researchers shifted their focus to combination therapies and targeting other signaling pathways that are in crosstalk with the MAPK pathway. One of the pathways that are reported to have consistent crosstalk with the MAPK pathway is Hedgehog-Gli (HH-Gli) signaling pathway [3], making it a potential new strategy for melanoma therapy improvement. Abnormal HH-Gli pathway activation has been described in a variety of human cancer types, including medulloblastoma, pancreatic, prostate, colon, breast, ovarian, and lung cancer [4–10]. The importance of the HH-Gli signaling pathway in melanoma and its resistance to therapy has also been noticed and reported. For example, studies show that inhibition of the HH-Gli pathway can suppress the growth of melanoma cells in vitro and in vivo. Furthermore, it has been demonstrated that Gli downregulation induced apoptosis and that this may contribute to the increased sensitivity of melanoma cells to vemurafenib [11–14]. However, identifying Gli transcriptional targets in melanoma can provide insight into the role of HH-Gli signaling in the pathogenesis of this tumor. The main effectors of HH-Gli signaling are Gli transcription factors (Gli1, Gli2, and Gli3). They can act as transcriptional activators or repressors; Gli2 and Gli3 harbor an N-terminal repressor domain and can act as both activators and repressors of the pathway, while Gli1, lacking this domain, acts only as a transcriptional activator [15]. In addition, one study identified Gli3 as an effector of KRAS/PI3K/AKT1 signaling in cancer cells [16]. There are two types of HH-Gli pathway activation: canonical and non-canonical. MAPK and PI3K can non-canonically activate the HH-Gli signaling pathway at the level of Gli transcription factors [3,17]. Previous research has already shown that MEK1/2-ERK1/2 signaling acts upstream of HH and regulates the activity of Gli transcription factors. For example, NRASQ61K and HRASV12G improve Gli1 function, increasing its transcriptional activity and nuclear localization [18]. Surprisingly, there are also studies reporting that the upstream members of the MAPK cascade, the mitogen-activated kinases MEKK1 and MEKK2/3, can negatively regulate Gli1 in medulloblastoma cells [19]. In order to find new Gli transcriptional targets that could be considered for combination therapy of melanoma, we performed RNA sequencing on melanoma cell lines with overexpressed Gli1, Gli2, and Gli3 and coupled the data with ChIP sequencing results on endogenous Gli1, Gli2, and Gli3 proteins for additional confirmation of direct Gli targets. Using these two methods, we have been able to confirm and validate 15 novel Gli targets that are involved in MAPK and many other signaling pathways, as revealed by pathway enrichment analysis.

2. Materials and Methods

2.1. Cell Lines

Ten human melanoma cell lines (A375, A375M, CHL-1, MEL224, MEL501, MEL505, MEWO, RPMI7951, SKMEL24, and SKMEL3) were kindly provided by Andreja Ambriović Ristov, PhD and Neda Slade, PhD. Cell lines HS895.SK (ATCC CRL-7636; Accession number CVCL_0992), HS895.T (ATCC CRL-7637; Accession number CVCL_0993), HS940.T (ATCC CRL-7691; Accession number CVCL_1038) and SKMEL2 (ATCC HTB-68; Accession number CVCL_0069) were purchased from the ATCC (Manassas, VA, USA). HS895.SK cell line represents a healthy control: skin keratinocytes isolated from the same patient as the HS895.T melanoma cell line. All cell lines were maintained in recommended medium: Dulbecco's Modified Eagle Medium (Merck KGaA, Darmstadt, Germany), RPMI 1640 medium (Merck KGaA, Darmstadt, Germany), or Eagle's Minimum Essential Medium (Merck KGaA, Darmstadt, Germany), supplemented with 10% FBS (Merck KGaA, Darmstadt, Germany), 1 mM sodium pyruvate, 1% streptomycin/penicillin and 4 mM L-glutamine (Gibco Thermo Fisher Scientific, Waltham, MA, USA).

2.2. Plasmids and Cell Transfection

For the *GLI* transfection experiments, cells were plated at density of 3×10^5 cells/well in 6-well plates, left to attach for 24 h, and then transfected with 5 µg of *GLI* expression plasmids: *GLI1* (pcDNA4NLSMTGLI1, kindly gifted by Fritz Aberger, PhD), *GLI2* and *GLI3* (p4TO6MTGLI2, pcDNA4/TO/GLI3richtig, both a kind gift from Milena Stevanović, PhD) using the X-fect reagent (Clontech, Mountain View, CA, USA) following the manufacturer's instructions.

2.3. MTT Assay

For determining cell viability and proliferation, compound 3-(4,5-Dimethylthiazol-2-yl)-2,5-diphenyltetrazolium bromide (MTT) was used as previously described [20]. Cells were treated with different HH-GLI pathway inhibitors using the concentration ranges that correspond to previously published studies: GANT61 5–25 µM (Selleck Chemicals, Houston, TX, USA), cyclopamine (CYC) 1.25–10 µM (Selleck Chemicals, Houston, TX, USA), and lithium chloride (LiCl) 5–40 mM (Kemika, Zagreb, Croatia) for 24–72 h [21–23]. Cell viability was measured on Labsystems Multiskan MS microplate reader (Thermo Fisher Scientific, Waltham, MA, USA) at 570 nm. The treatment was performed in quadruplicate for each dose, and the experiment was repeated twice.

2.4. Western Blot

Whole-cell protein extraction, determining the protein concentration, and western blot technique were performed as previously described [20]. The membranes were probed with following primary antibodies: rabbit anti-GLI1 1:300 (V812, Cell Signaling Technology, Danvers, MA, USA), mouse anti-GLI2 1:100 (sc-271786, Santa Cruz Biotechnology, Dallas, TX, USA), rabbit anti-GLI3 1:1000 (GTx104362, GeneTex, Irvine, CA, USA), rabbit anti-PTCH1 1:1000 (17520-1-AP, ProteinTech, Rosemont, IL, USA) and mouse anti-β-actin 1:4000 (60008-1-Ig, ProteinTech, Rosemont, IL, USA) was used as loading control. After overnight incubation, membranes were washed in TBST (Tris-Buffered Saline, 0.1% Tween® 20 Detergent) and incubated for 1 h with appropriate secondary HRP-conjugated antibodies, anti-rabbit 1:6000 (554021, BD Pharmingen, San Jose, CA, USA) and anti-mouse 1:8000 (554002, BD Pharmingen, San Jose, CA, USA). Proteins were visualized using SuperWest Signal Pico and Femto reagents (Thermo Fisher Scientific, Waltham, MA, USA) on Uvitec Image Alliance 4.7 instrument (UVItec, Cambridge, England, UK).

2.5. RNA-Sequencing

Human melanoma cell lines CHL-1 (wild-type for both NRAS and BRAF), MEL224 (NRAS^{Q61R}), and A375 (BRAF^{V600E}) were transfected with expression plasmids for *GLI1*, *GLI2* or *GLI3* in two independent experiments. Non-transfected lines were used as controls. Briefly, 200,000 cells were seeded in a Ø10 cm cell culture dish and transfected the next day with 5 µg of plasmid DNA, using the X-fect reagent (Clontech, Mountain View, CA, USA) and following the manufacturer's instructions. Forty-eight hours post-transfection, total RNA was isolated with Absolutely RNA miRNA Kit (Agilent Technologies, Santa Clara, CA, USA). The quality of the isolated RNA was checked on agarose gel, and RNA concentrations and purity were measured on NanoPhotometer N60 instrument (Implen, Munich, Germany). Sequencing libraries were generated and sequenced by DNA Link Company (Seoul, South Korea). The integrity of RNA samples was checked on Agilent 2100 Bioanalyzer (Agilent Technologies, Santa Clara, CA, USA). The instrument provided data on RNA concentration, electropherogram, rRNA subunit ratios, and RNA integrity number (RIN). All samples had RIN ≥ 8.0 and a 28S:18S ratio ≥ 1.4. Total amount of 1 µg of RNA was used. cDNA libraries were prepared using TruSeq mRNA library Kit, and sequencing was performed on Novaseq 6000 instrument (Illumina, San Diego, CA, USA).

2.6. Chromatin Immunoprecipitation Sequencing (ChIP-seq)

Chromatin immunoprecipitation was performed using SimpleChIP Plus Enzymatic Chromatin IP kit (Cat. no. #9005, Cell Signaling Technology, Danvers, MA, USA) following the manufacturer's protocol. Three cell lines with the strongest basal expression of GLI proteins were selected for the experiment (CHL-1, A375, and MEL224). Cells were cultured until 80–90% confluence in 150 cm² flasks. To preserve protein–DNA interactions, cells were fixed twice, first using 2 mM Di(N-succinimidyl) glutarate (DSG) (Merck KGaA, Darmstadt, Germany) followed by 1% formaldehyde. Samples were incubated with specific ChIP-grade antibodies against GLI1 10 µg/sample (AF3324, R&D Systems, Minneapolis, MN, USA) [24], GLI2 4 µg/sample (AF3526, R&D Systems) [24], and GLI3 10 µg/sample (AF3690, R&D Systems) overnight. Library preparation for next-generation sequencing was performed using SimpleChIP ChIP-seq DNA Library Prep Kit for Illumina (Cat. no. #56795, Cell Signaling Technology) and SimpleChIP ChIP-seq Multiplex Oligos for Illumina (Dual Index Primers) (Cat. no. #47538, Cell Signaling Technology) according to manufacturer's protocol. Libraries were prepared for 24 samples which included selected three cell lines for each GLI transcription factor with INPUT control in biological duplicates. A total of 5 ng of purified chromatin was used for each library preparation, followed by adaptor ligation. Samples were then purified from unbound adaptors using magnetic AMPure XP beads (Beckman Coulter, Brea, CA, USA), eluted, and amplified with a unique combination of dual index primers. Amplified chromatin fragments were additionally purified using magnetic beads. Quality control was performed on Bioanalyzer 2100 (Agilent Technologies, Santa Clara, CA, USA) and Qubit V1 (Invitrogen Thermo Fisher Scientific, Waltham, MA, USA). Next-generation sequencing was completed on NextSeq 500 (Illumina, San Diego, CA, USA).

2.7. Bioinformatic Analysis of RNA-seq Data

FastQC software (v.0.11.5) was used to assess the sequencing quality of the raw fastq data. The sequencing reads have been trimmed from adapters with Trim galore (v.0.3.7) and then mapped to human genome hg38 with STAR aligner (v.2.4.0d) with the following parameters: sjdbOverhang 99, outFilterMismatchNoverReadLmax 0.04, outFilterMultimapNmax 500, outSAMmultNmax 1. Mapped reads were then quantified with RSEM (v.1.2.26) over hg38 gencode transcriptome (v.28). Further analysis was performed with R (v.4.0.1), and differential gene expression was performed with edgeR (v.3.30.3) for each cell line with overexpressed GLI against the control. Gene Set Enrichment Analysis of KEGG pathways was performed with function gseKEGG from R package clusterProfiler (v.3.0.4). Data were visualized in R with custom scripts, available at <https://github.com/NenBarto/GLI> (accessed on 10 August 2022).

2.8. Bioinformatic Analysis of ChIP-seq Data

ChIP-seq libraries were first trimmed with trimgalore from FastQC (v.0.11.5) and mapped with BWA v0.7.9a to human genome hg38. After removing duplicates with picard-tools (v. 1.138), peaks were called with MACS (v.2.0.10) with parameters -f BAMPE -g -B -q 0.01. Further analysis was performed in R (v.4.0.1) and packages ChIPpeakAnno and ChIPseeker using custom scripts available at <https://github.com/NenBarto/GLI> (accessed on 10 August 2022). Motif enrichment was performed with MEME Suite v.5.3.0 [25]. The lists of differentially expressed genes (DEGs) identified by RNA-seq (FDR < 0.01, logFC > 1) were compared with the ChIP-seq identified lists of targets for each of the GLI proteins using the Venny 2.1 tool [26] and identified overlapping targets were selected for qPCR validation. DEGs for each of the GLI proteins were analyzed using the GeneAnalytics platform [27] to examine their involvement in different pathways and diseases. The targets that showed high fold change values, association with a large number of cancers, and involvement in the MAPK signaling pathway were selected for qPCR validation.

2.9. Quantitative PCR Analysis

Total RNA was extracted using TRIzol reagent (Invitrogen, Carlsbad, CA, USA) following the manufacturer's instructions. cDNA was generated from 1 µg of RNA using the High-Capacity cDNA synthesis kit (Thermo Fisher Scientific, Waltham, MA, USA) and qRT-PCR performed on CFX-96 instrument (Bio-Rad Laboratories, Hercules, CA, USA) using SsoAdvanced SYBR Green Supermix (Bio-Rad Laboratories, Hercules, CA, USA) with gene-specific primers. Fold change was calculated relative to the *RPLP0* and *TBP* housekeeping genes. Primer sequences used for qPCR are listed in Supplementary Table S1.

2.10. Statistical Analysis

D'Agostino–Pearson test was used for testing normality of data distribution. Non-normal data were log-transformed. An independent samples T-test or One-way ANOVA with Dunnett's post hoc test was used for inferring the differences in gene expression. Statistical analyses were performed with MedCalc v19.2.1 (MedCalc Software bv, Ostend, Belgium). Two-tail *p*-values < 0.05 were considered statistically significant.

3. Results

3.1. HH-GLI Signaling Pathway in Melanoma Cell Lines with Different Genetic Background and Their Response to Pathway Inhibition

In order to confirm HH-GLI pathway activation in melanoma cell lines, we analyzed relative gene and protein expression levels of the pathway components (*GLI1*, *GLI2*, *GLI3*, and *PTCH1*) on a panel of 14 human melanoma cell lines with different genetic backgrounds. Five cell lines (HS 895.SK, MEWO, CHL-1, HS 895.T, and MEL501) are wild-type for both *BRAF* and *NRAS* gene; five cell lines (RPMI7951, SKMEL24, SKMEL3, A375M, and A375) have a *BRAF*^{V600E} mutation; three cell lines (HS 940.T, SKMEL2, and MEL224) have an *NRAS*^{Q61R} mutation, and the MEL505 cell line has a *KRAS*^{G12V} mutation. Figure 1A shows that *PTCH1*, which is considered the direct target of HH-GLI signaling, is detected in all cell lines. On the other hand, protein levels of *GLI1*, *GLI2*, and *GLI3* are not detected equally in all melanoma cell lines. The highest expression levels of all three GLI proteins are detected in CHL-1, MEL501, A375, and MEL224 cell lines. *GLI3* shows the most consistent expression in all cell lines in the full-length form (*GLI3FL*), while in some cell lines, it can also be found in the repressor form (*GLI3R*). Other authors have also detected the expression of GLI proteins in some of the melanoma cell lines we used in our study (MEWO, SKMEL2, MEL501, SKMEL3, and RMPI-7951) [28]. *BRAF* or *NRAS* mutation status is not correlated with the differences in protein or gene expression between the cell lines, but *KRAS* mutated MEL505 cell line shows lower gene expression levels for all tested genes (Supplementary Figure S1). Out of the three *GLI* genes, *GLI3* shows the highest average gene expression among all groups, regardless of the mutational status (Figure 1B). Interestingly, cell line HS895.SK, which represents a healthy skin fibroblast control, showed no significant differences in gene expression levels compared to other melanoma cell lines, yet none of the analyzed proteins could be detected in this cell line. To test our hypothesis that in melanoma, activation of the HH-GLI signaling pathway is non-canonical due to its crosstalk with other signaling pathways, such as the MAPK pathway, we investigated how three HH-GLI pathway inhibitors (GANT61, CYC, and LiCl) affect cell viability and proliferation on 14 melanoma cell lines with different *BRAF* or *NRAS* mutation status (Figure 1C). Although we expected that cell lines with the highest expression of GLI proteins would be affected by the inhibition, this was not the case in our study. MTT assay showed that out of three HH-GLI inhibitors, the most effective is GANT61, a known direct GLI protein inhibitor. Cyclopamine, as an inhibitor of SMO, a membrane component of the canonical HH-GLI pathway activation, seems to have no or very little effect on the viability of melanoma cells, regardless of the dose increase or duration of the treatment (Figure 1C). We noticed that *BRAF*^{V600E} mutated cell lines seem to be more sensitive to GANT61 than cell lines that are wild-type for these genes, but in our case, this difference is not statistically significant (Supplementary Figure S2A). Additionally, we noticed a trend

for higher sensitivity of metastatic cell lines to GANT61 compared to primary tumor cell lines, but again, the results are not statistically significant (Supplementary Figure S2B). In conclusion, the response to GANT61, a GLI inhibitor, compared to the poor response to cyclopamine, a SMO inhibitor, supports non-canonical HH-GLI pathway activation in melanoma cell lines.

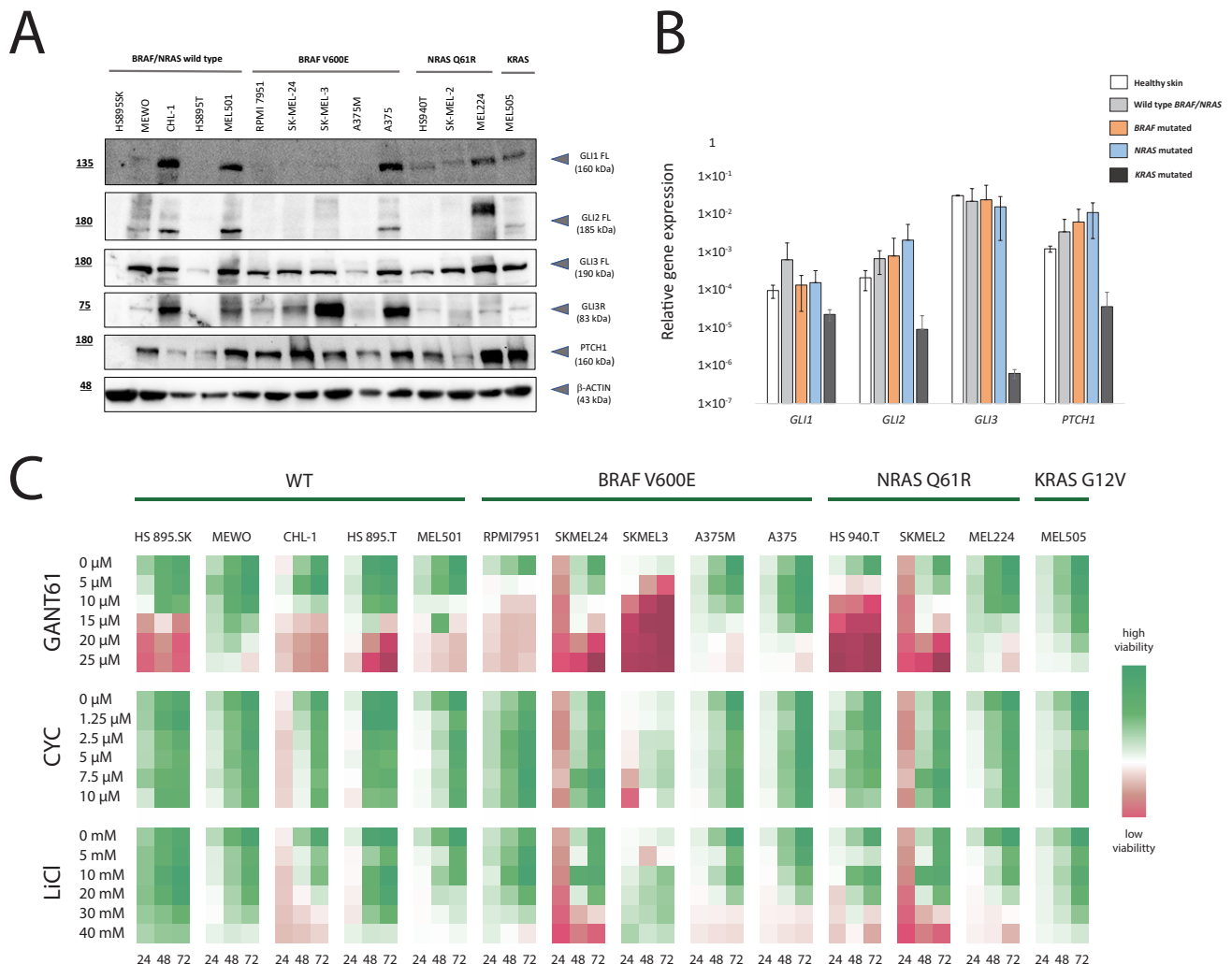


Figure 1. HH-GLI pathway activity in melanoma cell lines. **(A)** Western blot analysis of relative protein expression levels of GLI1, GLI2, GLI3 and PTCH1 in a panel of 14 melanoma cell lines. FL refers to the full-length protein, while R refers to the repressor form. **(B)** Average gene expression of *GLI1*, *GLI2*, *GLI3* and *PTCH1* relative to the housekeeping gene *RPLP0* summarized according to the mutational background of the tested panel of melanoma cell lines. **(C)** Heatmap showing MTT proliferation assay on 14 melanoma cell lines. Cells were treated with three different HH-GLI pathway inhibitors in five doses, during 24, 48 and 72 h. Green color indicates high cell viability and red color indicates low viability (cell death). The uncropped blots are shown in File S1.

3.2. RNA Sequencing Reveals Unique and Overlapping Targets of GLI Transcription Factors

As the first step in identifying novel GLI transcriptional targets that are in crosstalk with MAPK or other signaling pathways dysregulated in melanoma and that could be considered for combination therapy, we performed RNA sequencing on melanoma cell lines with overexpressed GLI1, GLI2, and GLI3 (Figure 2A and Supplementary Figure S3 show MDS plots). To our knowledge, there is no extensive data on the targets of all three GLI proteins in melanoma and their overlap. One study showed GLI1 and GLI2 transcriptional targets in primary neoplastic chondrocytes, detected by ChIP-seq and microarray methods,

but in this study, only three targets were validated by qPCR [24]. Thus far, no one has taken into consideration transcriptional targets of all three GLI proteins. Across all cell lines, we found 1642 targets that were overlapping for GLI1 and GLI2, 23 overlapping targets of GLI2 and GLI3, and only 9 overlapping targets of GLI1 and GLI3. In total, we found 150 GLI1, GLI2, and GLI3 overlapping targets (Figure 2B). There were 607 unique targets of GLI1, 1080 unique targets of GLI2, and 37 unique targets of GLI3. After filtering according to $FDR < 0.01$, we identified a total of 808 DEGs (631 upregulated, 183 downregulated) for GLI1. For GLI2, we found 941 DEGs (711 upregulated, 230 downregulated). For GLI3, there were only 58 DEGs (35 upregulated and 23 downregulated) found using this method (Supplementary Tables S2 and S3). Top scoring DEGs across all three cell lines are shown in Figure 2C. To identify pathways that are significantly represented in our list of differentially expressed genes, we performed pathway enrichment analysis. Figure 2D shows that some of the most enriched pathways in the case of GLI1 and GLI2 overexpression are Wnt signaling pathway, MAPK signaling pathway, and Ras signaling pathway. About 20–30% of DEGs are involved in these signaling pathways. An even bigger percentage of genes (30–40%) show involvement in Neuroactive ligand–receptor interactions. There is also significant involvement of DEGs in different cancer types (Figure 2D, Supplementary Figure S4). Our findings confirm the crosstalk of HH-GLI with other signaling pathways, and to our knowledge, this is the first study that considered transcriptional targets of all three GLI proteins in melanoma.

3.3. Chromatin Immunoprecipitation (ChIP) Sequencing Reveals Novel Binding Targets of GLI Proteins

ChIP sequencing was used to identify GLI1, GLI2, and GLI3 binding regions in human melanoma cell lines and to further confirm RNA-seq results. For this purpose, cell lines with the highest endogenous GLI protein expression levels (CHL-1, A375, and MEL224) were selected. ChIP-seq datasets were merged across cell lines to observe overall GLI binding sites and increase the signal-to-noise ratio. More than 80% of ChIP-seq peaks were identified in the intergenic regions (Figure 3A,B), which corresponds to their previously observed enhancer binding properties [29]. Overall, the three TFs shared most of the sites, with GLI2 containing the largest number of unique binding loci (Figure 3C). We identified 2183 genes that contained GLI TFs binding sites in their promoters: 527 for GLI1 (24%), 1103 for GLI2 (50%), and 553 for GLI3 (25%) (Figure 3C). As expected, only a small proportion of genes had all three GLI TFs in their promoter regions (157 out of 2183, 7.2%), with a much larger proportion of GLI3-specific promoter binding (35.8%) (Supplementary Table S4). The binding sites for GLI TFs were centered around the gene transcription start sites (Figure 3D) and were enriched for previously established motifs for GLI1 (MA1990.1), GLI2 (MA0734.1), and GLI3 (MA1491.1), with p -values of 4.71×10^{-61} , 8.4×10^{-7} and 1.64×10^{-75} , respectively. *PTCH1*, as a known target, showed two peaks in the transcriptional start site (TSS), which was previously reported for GLI2 [30], and its position corresponds to the H3K4me3 region. One of the newly identified target genes, *EBI3*, shows a broad peak in the promoter region of the gene (Figure 3E).

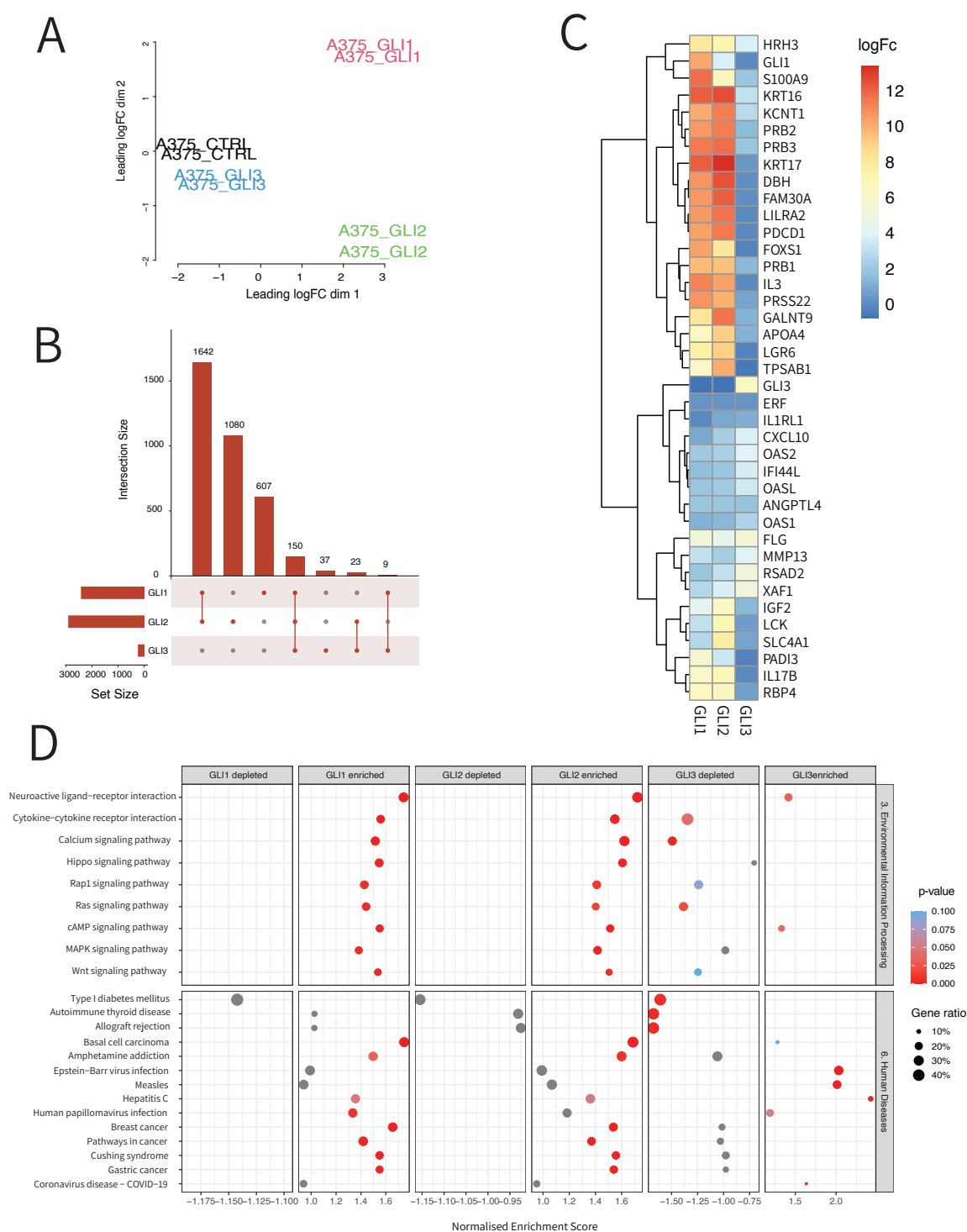


Figure 2. Expression profiles of CHL-1, A375, and MEL224 cell lines with transfected *GLI1*, *GLI2* and *GLI3*. **(A)** MDS plot of A375 cell line. **(B)** Upset plot of differentially expressed genes across all cell lines and GLI proteins. **(C)** Heatmap of expression of top DEGs sorted by logFC across all cell lines. **(D)** Gene enrichment analysis of DEGs across cell lines, transfection with GLI1-3 vs. control. Upper half of the plot shows KEGG pathway analysis, while the lower part shows categories of diseases. On x-axis: normalized enrichment scores. Size of the circles denote ratio of DE genes in pathways. Color denotes significance, with gray and blue circles denoting non-significant enrichments and red denotes significant enrichment.

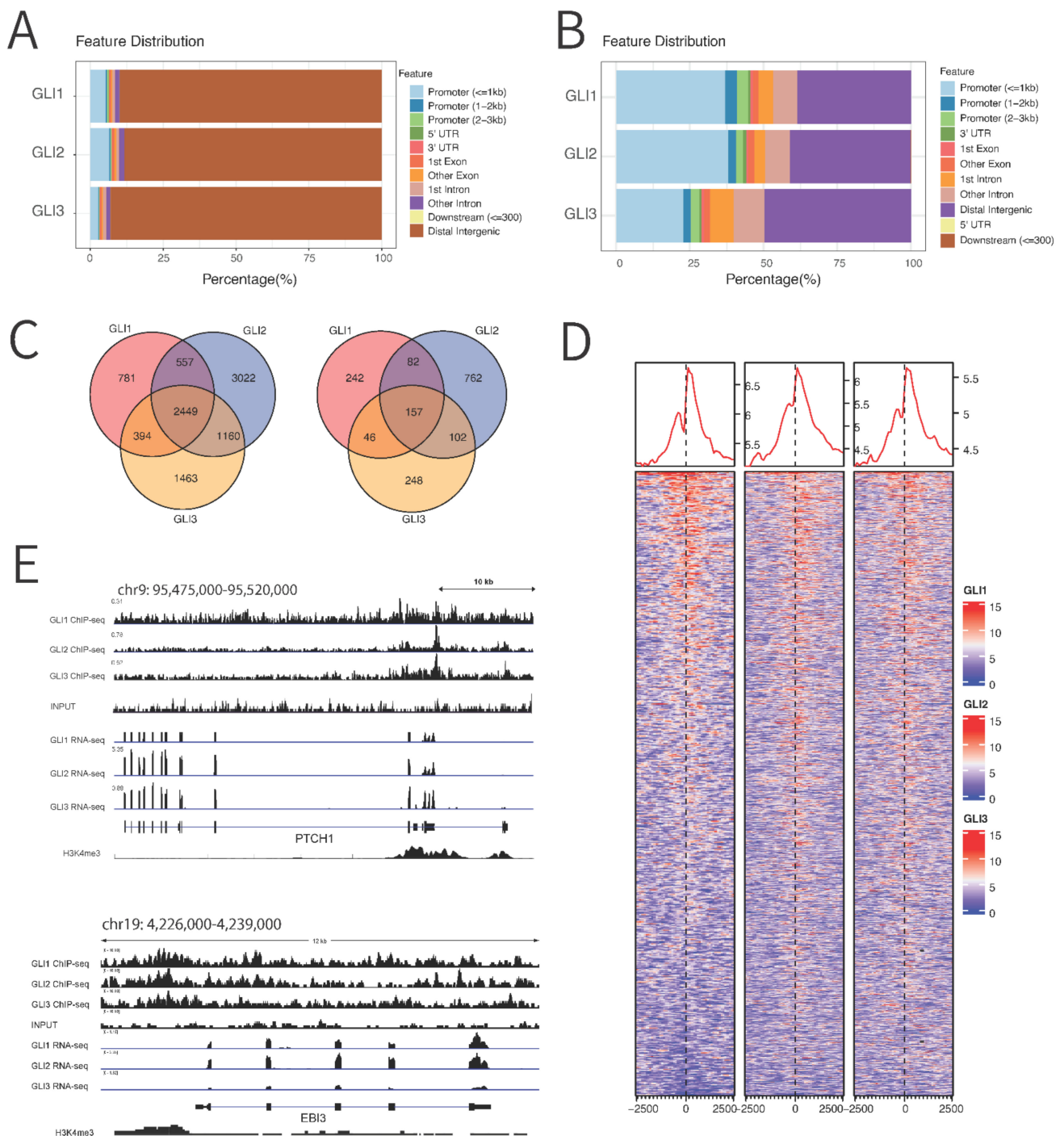


Figure 3. ChIP-seq analysis of GLI1–3 binding across cell lines. **(A)** Binding of peaks on the whole genome. **(B)** Binding of peaks that centered on the promoter regions **(C)** Overlap of GLI1–3 binding sites: left image shows overlapping of peaks on whole genome, and right image shows overlapping of peaks on the promoter regions only. FDR value was set to 0.2. **(D)** Heatmap of binding of GLI1–3 TFs across promoter sites. **(E)** Peak distribution in *PTCH1* and *EBI3* loci.

3.4. qPCR Validation of RNA Sequencing and ChIP Sequencing Data Confirms 15 Novel GLI Target Genes

To validate the biological reproducibility of the results of DEG analysis, we performed qPCR experiments on seven melanoma cell lines. Cell lines were chosen to represent the different mutational backgrounds: A375 (BRAF^{V600E} homozygous), SKMEL24 (BRAF^{V600E} heterozygous), MEL224 (NRAS^{Q61R} homozygous), SKMEL2 (NRAS^{Q61R} heterozygous),

MEL505 (KRAS^{G12V} heterozygous), CHL-1 and MEWO (wild-type for BRAF and NRAS). Selected cell lines were transfected with *GLI1*, *GLI2*, or *GLI3* expression plasmids, and gene expression of a total of 23 genes (21 novel targets, plus *PTCH1* and *GLI1* as known targets) was determined. To narrow down a list of targets for qPCR validation, two approaches were used (Figure 4A). The first approach identified potential targets under direct transcriptional control of GLI proteins by comparing the list of DEGs obtained by RNA-seq with the list of genes identified by ChIP-seq analysis for all three cell lines. For *GLI1*, 808 DEGs were compared with 231 identified ChIP-seq *GLI1* targets, identifying three common targets, namely: *FLG*, *SAMMSON*, and *SPRY2*. For *GLI2*, 941 DEGs were compared with 470 ChIP-seq *GLI2* targets, identifying 11 common targets: *HES1*, *EBI3*, *CACNA2D2*, *LAPTM5*, *LY6D*, *FLG*, *GLI1*, *PTCH1*, *RDH10*, *STK32C*, and *RAB34*. Among the identified targets, there were two known HH-GLI pathway targets (*PTCH1* and *GLI1*), confirming the validity of the selection process. A comparison of *GLI3* RNA-seq and ChIP-seq data showed no common targets. The ChIP-seq analysis identified *GLI1* or *GLI2* binding motifs in all 11 identified targets, suggesting they are direct transcriptional targets of *GLI1* and/or *GLI2* proteins. The second approach was to analyze the DEGs from RNA-seq independently of the ChIP-seq data to identify potential indirect targets. After filtering by FDR and logFC values, the GeneAnalytics tool of the GeneCards database (genecards.org, RRID:SCR_002773) was used to identify the role of DEGs in signaling pathways and diseases. Several categories of pathways and diseases with a high relevance score were considered when selecting genes of interest: “Pathways in cancer”, “PI3K-AKT signaling pathway”, “MAPK signaling pathway”, “WNT/Hedgehog/NOTCH”, “neoplasm”, “melanoma” and “abnormalities of the skin”, as well as logFC values of these genes in RNA-seq analysis. Additional screening was performed based on their expression in melanoma from the GEPIA database [31] (SKCM dataset vs TCGA normal and GTEx data, N(T) = 461, N(N) = 558) and The Human Protein Atlas (proteintatlas.org) [32] (RNA expression and staining of melanoma) as well as survival data from GEPIA database. With this approach, we were able to identify ten targets: *KRT16*, *KRT17*, *S100A7*, *S100A9*, *GH1*, *SOX9*, *BIRC7*, *MRAS*, *RET*, and *IL1R2*. Finally, 21 targets were selected for qPCR validation: 10 identified by RNA-seq only (*KRT16*, *KRT17*, *S100A7*, *S100A9*, *GH1*, *SOX9*, *BIRC7*, *MRAS*, *RET* and *IL1R2*) and 11 targets identified with both ChIP-seq and RNA-seq (*HES1*, *FLG*, *RAB34*, *SAMMSON*, *SPRY2*, *CACNA2D2*, *LAPTM5*, *LY6D*, *RDH10*, *STK32C* and *EBI3*) (Figure 4B,C). A summary of known functions of these targets and their role in cancer is shown in Table 1. Identified targets, including *KRT16*, *KRT17*, *S100A7*, *MRAS*, *BIRC7*, *IL1R2*, as well as several direct GLI targets (confirmed by both RNA-seq and ChIP-seq)—*RAB34*, *LAPTM5*, *RDH10*, and *STK32C*—exhibited a consistent and uniform expression pattern. In addition, the genes *EBI3*, *GH1*, *SOX9*, *RET*, and *SPRY2* are also good candidates for HH-GLI targets but exhibited a less uniform expression pattern in these melanoma cell lines. Overall, by combining RNA-seq and ChIP-seq results and elaborate filtering of these genes, we successfully validated 15 novel targets of GLI proteins in melanoma cell lines.

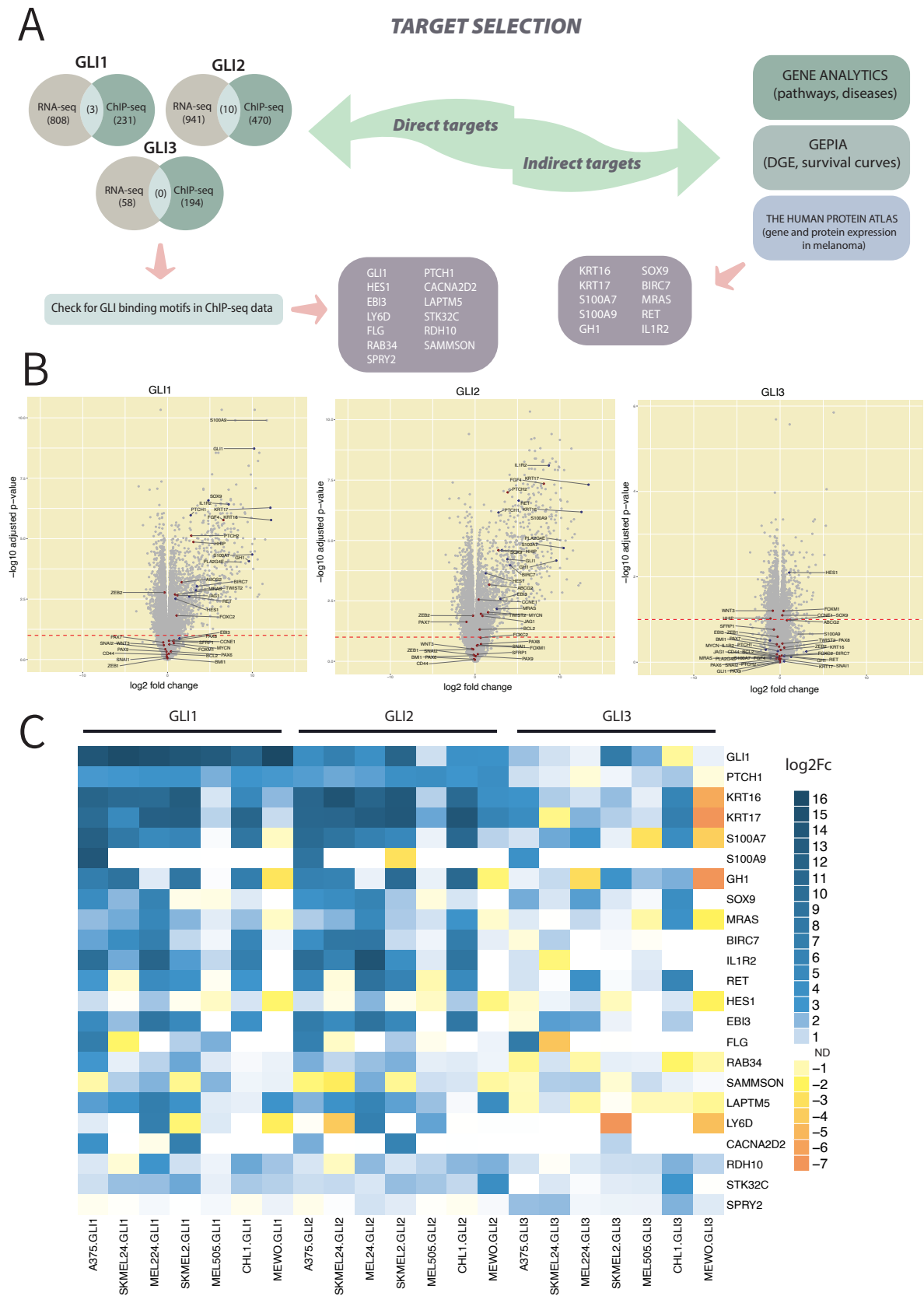


Figure 4. Validation of 21 selected DEGs. (A) Schematic representation of choosing DEGs for qPCR validation. (B) Volcano plot represents previously identified targets of HH-GLI signaling in red and targets selected for validation in this study in blue for each GLI protein. (C) Heatmap showing qPCR

validation of GLI target genes identified by both ChIP-seq and RNA-seq on seven melanoma cell lines (A375, SKMEL24, MEL224, SKMEL2, MEL505, CHL-1 and MEWO) with overexpressed GLI1, GLI2 or GLI3. The experiment was repeated two times in triplicates. Validation was performed for 21 DEGs and two known pathway targets *PTCH1* and *GLI1* as controls. The relative expression level of each gene was determined using the $2^{-\Delta\Delta C_t}$ method with *RPLP0* as the internal reference gene. Heatmap shows log2 fold change values, ND stating that expression levels could not be detected after 37th cycle.

Table 1. Summary of known functions and roles of 21 selected GLI target genes in cancer.

Gene	Function According to Gene Cards	Role in Cancer	Reference
<i>KRT16</i>	type I keratin that regulates innate immunity in response to skin barrier breach	regulates immune response, metastasis, cancer stemness and drug resistance in melanoma, SCC, and breast cancer	[33–36]
<i>KRT17</i>	type I keratin involved in regulation of protein synthesis and epithelial cell growth	regulates therapy resistance, proliferation, migration and invasion in CRC, pancreatic cancer, and NSCLC	[37–40]
<i>S100A7</i>	member of the S100 family of proteins involved in the regulation of cell cycle and differentiation	regulates tumor invasion, angiogenesis, migration, EMT and chemoresistance in melanoma, cervical cancer, and ovarian cancer	[41–45]
<i>S100A9</i>	calcium- and zinc-binding protein involved in immune response	regulates chemoresistance, cell invasion and metastasis in melanoma, cervical carcinoma, and prostate cancer	[46–49]
<i>GH1</i>	member of the somatotropin/prolactin family of hormones important for growth control	dysregulates MAPK pathway and blocks cell motility in colon cancer	[50]
<i>SOX9</i>	transcription factor important for differentiation and skeletal development	regulates metastasis, cell invasion, migration and stemness in melanoma, CRC, and esophageal cancer	[51–54]
<i>MRAS</i>	Ras GTPase that functions as signal transducer in cell growth and differentiation	regulates MAPK pathway and drives tumorigenesis in gastric cancer and prostate cancer	[55–57]
<i>BIRC7</i>	member of the inhibitor of apoptosis protein family associated with cancer progression and chemotherapy resistance	regulates chemoresistance and can serve as a biomarker in prostate cancer, melanoma, and lung cancer	[58–66]
<i>IL1R2</i>	cytokine receptor that belongs to the interleukin 1 receptor family	regulates proliferation, angiogenesis and tumorigenesis initiation in breast cancer, melanoma, gastric cancer, and CRC	[67–71]
<i>RET</i>	receptor tyrosine-protein kinase involved in cell proliferation, migration, and differentiation	RET fusion are associated with tumorigenesis of chronic myelomonocytic leukemia	[72]
<i>HES1</i>	transcriptional repressor involved in cell differentiation, cell cycle, apoptosis, and self-renewal	regulates cell proliferation, invasion and self-renewal in CRC, breast cancer and glioblastoma	[73–76]
<i>EBI3</i>	secretory glycoprotein belonging to the hematopoietin receptor family involved in IL-27 formation	EBI3 overexpression is associated with poor prognosis of breast and cervical cancer and impaired immune response in melanoma	[77–80]
<i>FLG</i>	intermediate filament-associated protein that aggregates keratin intermediate filaments in mammalian epidermis	regulates growth and angiogenesis and can be valuable in prognosis and treatment of melanoma	[81,82]
<i>RAB34</i>	small GTPase involved in protein transport and ciliogenesis pathways	regulates cell adhesion, migration and invasion in breast cancer and correlates with tumor progression of HCC and glioma	[83–85]
<i>SAMMSON</i>	lncRNA with crucial role in cell survival and mitochondrial metabolism	regulates therapy response and mitochondrial function in melanoma	[86,87]

Table 1. Cont.

Gene	Function According to Gene Cards	Role in Cancer	Reference
<i>LAPTM5</i>	transmembrane receptor associated with lysosomes	potential biomarker for HCC, glioblastoma, and testicular cancer	[88–90]
<i>LY6D</i>	marker at earliest stage specification of lymphocytes between B-and T-cell development	therapy outcome and survival prediction in BCC, prostate cancer, NSCLC, laryngeal cancer, and breast cancer	[91–95]
<i>CACNA2D2</i>	alpha-2/delta subunit of the voltage-dependent calcium channel complex	regulates cell proliferation and angiogenesis in prostate cancer, while CACNA2D2 inhibition induces NSCLC tumorigenesis	[96,97]
<i>RDH10</i>	retinol dehydrogenase essential for organ development	RDH10 overexpression has an antiproliferative effect in hepatocellular carcinoma	[98]
<i>STK32C</i>	serine/threonine protein kinase	STK32C overexpression in bladder cancer contributes to tumor progression	[99]
<i>SPRY2</i>	inhibitor of RTK signaling proteins activity	SPRY2 inhibits cell growth and therapy resistance occurrence via MAPK pathway in melanoma and hepatocellular carcinoma	[100–102]

4. Discussion

BRAF inhibitors have improved patient survival compared with standard chemotherapy, but these benefits are not persistent, as most patients develop resistance to therapy which leads to disease progression [103]. There are different mechanisms that can activate a variety of signaling pathways, thereby bypassing the effect of BRAF inhibition. It is already known that the HH-GLI signaling pathway is active in melanoma [11,12,28,104]. Here, we confirm HH-GLI pathway activity in 14 melanoma cell lines with different genetic backgrounds. Several studies also show that inhibition of the HH-GLI pathway can decrease melanoma cell proliferation [11,12,105–107]. The HH-GLI pathway inhibitors affect signal transduction at different levels. Cyclopamine inhibits the SMO protein on the cell membrane [108]. In contrast, lithium chloride increases the phosphorylation of Ser9 residue on GSK3 β kinase, which regulates GLI protein activity at the post-translational level. GSK3 β phosphorylates GLI3 and thereby promotes its processing into GLI3R, which downregulates the HH-GLI pathway [109]. ATO and GANT61, in turn, affect the activity of GLI proteins [110,111]. One of these studies pointed out that primary melanoma cell lines with *BRAF* mutation are more sensitive to SMO inhibitor, sonidegib, than *BRAF* wild-type cells [11]. We also noticed that BRAF^{V600E} mutated cell lines seem to be more sensitive to inhibitor GANT61 than cell lines that are wild-type for these genes, but in our case, this difference is not statistically significant. Thus far, studies have demonstrated that in colon cancer, neuroblastoma, and pancreatic cancer, GANT61 is the most effective inhibitor of cell growth among all tested HH-GLI inhibitors [112–114]. On the other hand, one study in melanoma shows comparable effects of GANT61 and cyclopamine [115]. Our MTT-assay results show that cyclopamine seems to have no or very little effect on the viability of melanoma cell lines, while the most effective inhibitor in melanoma cell lines was, indeed, GANT61. This result also supports the assumption that, in the case of melanoma, non-canonical pathway activation is likely more important than canonical [3,19,104,107].

Because the exact interplay between the HH-GLI pathway and MAPK signaling pathway is not yet understood, we decided to investigate the transcriptional targets of all three GLI proteins in melanoma with different genetic backgrounds, either harboring a *BRAF* mutation, an *NRAS* mutation, or no mutation in these two genes. We applied RNA sequencing and combined it with ChIP sequencing to identify direct but also unique and overlapping targets of GLI1, GLI2, and GLI3 in three melanoma cell lines. By doing so, we identified a total of 808 DEGs for GLI1, 941 DEGs for GLI2, and 58 DEGs for GLI3. KEGG analysis confirmed that many of the identified DEGs are involved in various signaling pathways, including MAPK, Ras, Hippo, and Wnt pathways [3,116], as well as in many

types of cancer [8,117–119]. Our next step of carefully screening and filtering targets led us to select 21 targets for qPCR validation. We successfully validated 15 novel targets of GLI proteins that were not identified in any previous study. To our knowledge, this is the first comprehensive study of transcriptional targets of all three GLI proteins in melanoma. Identified targets, such as *KRT16*, *KRT17*, *S100A7*, *MRAS*, *BIRC7*, *IL1R2*, as well as several direct GLI targets (confirmed by both RNA-seq and ChIP-seq)—*RAB34*, *LAPTM5*, *RDH10*, and *STK32C*—have a consistent and uniform expression pattern. Expression levels of these genes are increased with GLI1 or GLI2 overexpression, regardless of the mutational status of the cell lines. We were also able to validate genes *EBI3*, *GH1*, *SOX9*, *RET*, and *SPRY2* as HH-GLI targets. Their expression was consistent in the majority of the cell lines, with few exceptions. Six targets—*S100A9*, *FLG*, *SAMMSON*, *LY6D*, *CACNA2D2*, and *HES1*—were found to have variable expression in different melanoma cell lines, so they could not be validated as GLI targets in melanoma.

Table 1 represents a summary of protein functions and already published roles in cancer for 21 discovered GLI targets. Thus far, 8 out of 21 GLI targets we chose to validate—*KRT16*, *S100A9*, *SOX9*, *BIRC7*, *EBI3*, *FLG*, *SAMMSON* and *SPRY2*—were already implicated in melanoma pathogenesis [34,46,47,51,52,64,79,81,82,87,101,120]. *KRT16*, a regulator of innate immunity in the skin, seemed to be significantly downregulated in metastatic melanoma and was also found to be the highest discriminator between prognostic and metastatic melanoma [34]. Our RNA-seq and qPCR results show that out of all targets, *KRT16* is by far the most upregulated overlapping target of GLI1 and GLI2, with a logFC value of 12.5 obtained by RNA-seq and log2FC value that goes up to 16 in qPCR experiments, depending on the cell line. LogFC values and expression patterns of *KRT17* closely follow those of *KRT16* in all seven melanoma cell lines (Figure 4C).

S100A9 is suggested to have a role in acquired resistance to BRAF inhibitors [47] and in melanoma metastasis [46]. Our results show that *S100A9* is expressed only in one tested melanoma cell line, A375 (*BRAF*^{V600E} mut). In the majority of our melanoma cell lines, *S100A9* expression could not be detected. By contrast, *S100A7* shows a much wider expression pattern than *S100A9*, but despite its ability to promote cell proliferation, migration, invasion, and tumor metastasis in cervical, breast, and ovarian cancer [42–45], *S100A7* has not previously been implicated in melanoma pathogenesis. From other validated targets in this study that have not yet been investigated in melanoma, we would like to point out *MRAS*, *IL1R2*, *RAB34*, *LAPTM5*, *RDH10*, and *STK32C*. Similar to *S100A7*, we considered them important because of their involvement in processes of tumor cell proliferation, migration, and invasion, or their interactions with members of the MAPK cascade. For example, it is shown that cells overexpressing *MRAS* have higher migratory potential and that *MRAS*/SHOC2/SCRIB complex coordinates ERK pathway dynamics [56]. It has been proposed that increased *IL1R2* levels are important during the initiation and progression of human gastric cancer [70]. One study demonstrates the existence of a novel mechanism of tyrosine phosphorylation of *RAB34* in regulating cell migration, invasion, and adhesion through modulating the endocytosis, stability, and recycling of integrin $\beta 3$ [84]. It has been shown that inhibition of *LAPTM5* blocks bladder cancer cell proliferation and cell cycle via deactivation of ERK1/2 and p38 [121] and that silencing of *STK32C* inhibited tumor cell proliferation, migration, and invasion in human bladder cancer cells [99]. Finally, *RDH10* overexpression has an antiproliferative effect on hepatocellular carcinoma cell lines [98].

Although we identified *FLG* as the overlapping target of GLI1, GLI2, and GLI3 and detected it with both ChIP-seq and RNA-seq, its expression levels detected by qPCR experiments are not consistent between the cell lines. A375 cell line shows increased expression levels of *FLG* in all GLI overexpressed samples, while SKMEL24 shows a decrease in *FLG* expression levels. In the other cell lines, *FLG* expression could not be detected with qPCR. A previous study has noted the important role of the long noncoding RNA (lncRNA) *SAMMSON* in melanoma [86]. More recently, *SAMMSON* has been shown to be important for human melanoma cell growth and survival while also highlighting the role of a *SAMMSON* in modulating the adaptive resistance of mutant *BRAF* melanoma to

RAF inhibitors [87]. Similar to *SAMMSON*, *SPRY2* has also been implicated in resistance to BRAF inhibitors [101,120]. Our RNA-seq results reveal that both *SAMMSON* and *SPRY2* are downregulated targets of GLI1, and ChIP-seq confirms that *SAMMSON* has a GLI1 binding motif, while *SPRY2* contains GLI1 and GLI2 binding motifs. Because GLI1 is a transcriptional activator, it is not clear how it downregulates the expression of these two targets. It is likely that some other factors, apart from GLI1, play a role in their regulation. qPCR results show that *SAMMSON* expression levels vary among the cell lines. For example, A375 and SKMEL2 (with GLI1 or GLI2 overexpression) exhibit decreased expression levels of *SAMMSON*, while other cell lines, such as SKMEL24, MEL224, and MEL505, generally show increased *SAMMSON* expression levels. qPCR results show that *SPRY2* is detected in all melanoma cell lines, especially those with GLI3 overexpression.

5. Conclusions

Our studies confirm that in melanoma, the HH-GLI signaling pathway is in crosstalk with other signaling pathways and that its activation is more likely non-canonical than canonical. Out of 21 selected targets, we validated 15 as novel targets of GLI proteins, considering their expression in melanoma cell lines and possession of GLI binding motifs. Our study provides insight into the unique and overlapping transcriptional output of the GLI proteins in melanoma, which will contribute to a better understanding of the GLI code and its role in tumorigenesis. Other potential targets can also be functionally validated using this data in the future, especially by researchers in the HH-GLI field that are interested in other aspects of HH-GLI signaling. Our findings provide new potential targets to consider while designing melanoma-targeted therapy, especially in the case of recurrent disease due to therapy resistance.

Supplementary Materials: The following supporting information can be downloaded at: <https://www.mdpi.com/article/10.3390/cancers14184540/s1>, Table S1. List of all primers used for qPCR; Table S2. RNAseq_individual_lines; Table S3. RNAseq_all_lines; Table S4. ChIPseq; Figure S1. HH-GLI pathway activity in melanoma cell lines; Figure S2. GANT61 IC50 values; Figure S3. MDS plot; Figure S4. KEGG pathway analysis. File S1. Full pictures of the Western blots.

Author Contributions: M.K., N.P., N.B. and M.S. wrote the paper, M.S. designed and coordinated the study, M.K., N.P., T.P., J.Č. and V.M. conducted the experiments, P.O. and N.B. performed statistical and bioinformatics analysis, C.K. and M.S. secured the funding. All the authors participated in final proofreading of the paper. All authors have read and agreed to the published version of the manuscript.

Funding: This research was funded by the Croatian Science Foundation project IP-2018-01-4889 titled “Differential regulation of the GLI code in BRAF/NRAS driven tumors” and the Ideas grant 2004306 from the National Health and Medical Research Council (NHMRC) of Australia and DP210103811 from the Australian Research Council (ARC). The work of doctoral student NP has been supported by the “Young Researchers’ Career Development Project—Training of Doctoral Students” of the Croatian Science Foundation.

Data Availability Statement: Raw and processed RNA-seq and ChIP-seq sequencing data can be found in the ArrayExpress database under the following ID: E-MTAB-11936. Complete gene lists resulting from all analyses are provided as Supplementary Tables S2–S4.

Acknowledgments: We thank our colleagues Andreja Ambriović Ristov and Neda Slade for the cell lines, Fritz Aberger and Milena Stevanović for the constructs, and Oliver Vugrek, Filip Rokić and Dominik Kaczorowski for the help with sequencing.

Conflicts of Interest: The authors declare no conflict of interest.

References

1. Davis, L.E.; Shalin, S.C.; Tackett, A.J. Current State of Melanoma Diagnosis and Treatment. *Cancer Biol. Ther.* **2019**, *20*, 1366–1379. [CrossRef] [PubMed]
2. Davies, H.; Bignell, G.R.; Cox, C.; Stephens, P.; Edkins, S.; Clegg, S.; Teague, J.; Woffendin, H.; Garnett, M.J.; Bottomley, W.; et al. Mutations of the BRAF Gene in Human Cancer. *Nature* **2002**, *417*, 949–954. [CrossRef] [PubMed]

3. Rovida, E.; Stecca, B. Mitogen-Activated Protein Kinases and Hedgehog-GLI Signaling in Cancer: A Crosstalk Providing Therapeutic Opportunities? *Semin. Cancer Biol.* **2015**, *35*, 154–167. [[CrossRef](#)] [[PubMed](#)]
4. Raducu, M.; Fung, E.; Serres, S.; Infante, P.; Barberis, A.; Fischer, R.; Bristow, C.; Thézéas, M.-L.; Finta, C.; Christianson, J.C.; et al. SCF (Fbx17) Ubiquitylation of Sufu Regulates Hedgehog Signaling and Medulloblastoma Development. *EMBO J.* **2016**, *35*, 1400–1416. [[CrossRef](#)]
5. Berman, D.M.; Karhadkar, S.S.; Maitra, A.; Montes De Oca, R.; Gerstenblith, M.R.; Briggs, K.; Parker, A.R.; Shimada, Y.; Eshleman, J.R.; Watkins, D.N.; et al. Widespread Requirement for Hedgehog Ligand Stimulation in Growth of Digestive Tract Tumours. *Nature* **2003**, *425*, 846–851. [[CrossRef](#)]
6. Sheng, T.; Li, C.; Zhang, X.; Chi, S.; He, N.; Chen, K.; McCormick, F.; Gatalica, Z.; Xie, J. Activation of the Hedgehog Pathway in Advanced Prostate Cancer. *Mol. Cancer* **2004**, *3*, 29. [[CrossRef](#)]
7. Varnat, F.; Duquet, A.; Malerba, M.; Zbinden, M.; Mas, C.; Gervaz, P.; Ruiz i Altaba, A. Human Colon Cancer Epithelial Cells Harbour Active HEDGEHOG-GLI Signalling That Is Essential for Tumour Growth, Recurrence, Metastasis and Stem Cell Survival and Expansion. *EMBO Mol. Med.* **2009**, *1*, 338–351. [[CrossRef](#)]
8. Marini, K.D.; Payne, B.J.; Watkins, D.N.; Martelotto, L.G. Mechanisms of Hedgehog Signalling in Cancer. *Growth Factors* **2011**, *29*, 221–234. [[CrossRef](#)]
9. Ozretić, P.; Trnski, D.; Musani, V.; Maurac, I.; Kalafatić, D.; Orešković, S.; Levanat, S.; Sabol, M. Non-Canonical Hedgehog Signaling Activation in Ovarian Borderline Tumors and Ovarian Carcinomas. *Int. J. Oncol.* **2017**, *51*, 1869–1877. [[CrossRef](#)]
10. Giroux-Leprieur, E.; Costantini, A.; Ding, V.W.; He, B. Hedgehog Signaling in Lung Cancer: From Oncogenesis to Cancer Treatment Resistance. *Int. J. Mol. Sci.* **2018**, *19*, E2835. [[CrossRef](#)]
11. O'Reilly, K.E.; Vega-Saenz de Miera, E.; Segura, M.F.; Friedman, E.; Polisen, L.; Han, S.W.; Zhong, J.; Zavadil, J.; Pavlick, A.; Hernando, E.; et al. Hedgehog Pathway Blockade Inhibits Melanoma Cell Growth in Vitro and in Vivo. *Pharmaceuticals* **2013**, *6*, 1429–1450. [[CrossRef](#)]
12. Jalili, A.; Mertz, K.D.; Romanov, J.; Wagner, C.; Kalthoff, F.; Stuetz, A.; Pathria, G.; Gschaidner, M.; Stingl, G.; Wagner, S.N. NVP-LDE225, a Potent and Selective SMOOTHENED Antagonist Reduces Melanoma Growth In Vitro and In Vivo. *PLoS ONE* **2013**, *8*, e69064. [[CrossRef](#)]
13. Gunarta, I.K.; Li, R.; Nakazato, R.; Suzuki, R.; Boldbaatar, J.; Suzuki, T.; Yoshioka, K. Critical Role of Glioma-associated Oncogene Homolog 1 in Maintaining Invasive and Mesenchymal-like Properties of Melanoma Cells. *Cancer Sci.* **2017**, *108*, 1602–1611. [[CrossRef](#)]
14. Faião-Flores, F.; Alves-Fernandes, D.K.; Pennacchi, P.C.; Sandri, S.; Vicente, A.L.S.A.; Scapulatempo-Neto, C.; Vazquez, V.L.; Reis, R.M.; Chauhan, J.; Goding, C.R.; et al. Targeting the Hedgehog Transcription Factors GLI1 and GLI2 Restores Sensitivity to Vemurafenib-Resistant Human Melanoma Cells. *Oncogene* **2017**, *36*, 1849–1861. [[CrossRef](#)]
15. Sabol, M.; Trnski, D.; Musani, V.; Ozretić, P.; Levanat, S. Role of GLI Transcription Factors in Pathogenesis and Their Potential as New Therapeutic Targets. *Int. J. Mol. Sci.* **2018**, *19*, 2562. [[CrossRef](#)]
16. Lo Re, A.E.; Fernandez-Barrena, M.G.; Almada, L.L.; Mills, L.D.; Elswa, S.F.; Lund, G.; Ropolo, A.; Molejon, M.I.; Vaccaro, M.I.; Fernandez-Zapico, M.E. Novel AKT1-GLI3-VMP1 Pathway Mediates KRAS Oncogene-Induced Autophagy in Cancer Cells. *J. Biol. Chem.* **2012**, *287*, 25325–25334. [[CrossRef](#)]
17. Riobo, N.A.; Saucy, B.; DiLizio, C.; Manning, D.R. Activation of Heterotrimeric G Proteins by Smoothed. *Proc. Natl. Acad. Sci. USA* **2006**, *103*, 12607. [[CrossRef](#)]
18. Pietrobono, S.; Gagliardi, S.; Stecca, B. Non-Canonical Hedgehog Signaling Pathway in Cancer: Activation of GLI Transcription Factors Beyond Smoothed. *Front. Genet.* **2019**, *10*, 556. [[CrossRef](#)]
19. Antonucci, L.; Di Magno, L.; D'Amico, D.; Manni, S.; Serrao, S.M.; Di Pastena, F.; Bordone, R.; Yurtsever, Z.N.; Caimano, M.; Petroni, M.; et al. Mitogen-Activated Kinase Kinase Kinase 1 Inhibits Hedgehog Signaling and Medulloblastoma Growth through GLI1 Phosphorylation. *Int. J. Oncol.* **2018**, *54*, 505–514. [[CrossRef](#)]
20. Zubčić, V.; Rinčić, N.; Kurtović, M.; Trnski, D.; Musani, V.; Ozretić, P.; Levanat, S.; Leović, D.; Sabol, M. GANT61 and Lithium Chloride Inhibit the Growth of Head and Neck Cancer Cell Lines Through the Regulation of GLI3 Processing by GSK3β. *Int. J. Mol. Sci.* **2020**, *21*, E6410. [[CrossRef](#)]
21. Mazumdar, T.; DeVecchio, J.; Shi, T.; Jones, J.; Agyeman, A.; Houghton, J.A. Hedgehog Signaling Drives Cellular Survival in Human Colon Carcinoma Cells. *Cancer Res.* **2011**, *71*, 1092–1102. [[CrossRef](#)] [[PubMed](#)]
22. Wang, X.; Fang, Z.; Wang, A.; Luo, C.; Cheng, X.; Lu, M. Lithium Suppresses Hedgehog Signaling via Promoting ITCH E3 Ligase Activity and Gli1-SUFU Interaction in PDA Cells. *Front. Pharmacol.* **2017**, *8*, 820. [[CrossRef](#)] [[PubMed](#)]
23. Plaisant, M.; Giorgetti-Peraldi, S.; Gabrielson, M.; Loubat, A.; Dani, C.; Peraldi, P. Inhibition of Hedgehog Signaling Decreases Proliferation and Clonogenicity of Human Mesenchymal Stem Cells. *PLoS ONE* **2011**, *6*, e16798. [[CrossRef](#)] [[PubMed](#)]
24. Ali, S.A.; Niu, B.; Cheah, K.S.E.; Alman, B. Unique and Overlapping GLI1 and GLI2 Transcriptional Targets in Neoplastic Chondrocytes. *PLoS ONE* **2019**, *14*, e0211333. [[CrossRef](#)] [[PubMed](#)]
25. Bailey, T.L.; Johnson, J.; Grant, C.E.; Noble, W.S. The MEME Suite. *Nucleic Acids Res.* **2015**, *43*, W39–W49. [[CrossRef](#)] [[PubMed](#)]
26. Oliveros, J.C. Venny. An Interactive Tool for Comparing Lists with Venn's Diagrams. 2007. Available online: <https://Bioinfo.gp.Cnb.Csic.Es/Tools/Venny/Index.Html> (accessed on 10 August 2022).

27. Ben-Ari Fuchs, S.; Lieder, I.; Stelzer, G.; Mazor, Y.; Buzhor, E.; Kaplan, S.; Bogoch, Y.; Plaschkes, I.; Shitrit, A.; Rappaport, N.; et al. GeneAnalytics: An Integrative Gene Set Analysis Tool for Next Generation Sequencing, RNAseq and Microarray Data. *OMICS* **2016**, *20*, 139–151. [\[CrossRef\]](#)
28. Réda, J.; Vachtenheim, J.; Vlčková, K.; Horák, P.; Vachtenheim, J.; Ondrušová, L. Widespread Expression of Hedgehog Pathway Components in a Large Panel of Human Tumor Cells and Inhibition of Tumor Growth by GANT61: Implications for Cancer Therapy. *Int. J. Mol. Sci.* **2018**, *19*, 2682. [\[CrossRef\]](#)
29. Lex, R.K.; Ji, Z.; Falkenstein, K.N.; Zhou, W.; Henry, J.L.; Ji, H.; Vokes, S.A. GLI Transcriptional Repression Regulates Tissue-Specific Enhancer Activity in Response to Hedgehog Signaling. *eLife* **2020**, *9*, e50670. [\[CrossRef\]](#)
30. Yin, W.-C.; Satkunendran, T.; Mo, R.; Morrissy, S.; Zhang, X.; Huang, E.S.; Uusküla-Reimand, L.; Hou, H.; Son, J.E.; Liu, W.; et al. Dual Regulatory Functions of SUFU and Targetome of GLI2 in SHH Subgroup Medulloblastoma. *Dev. Cell* **2020**, *52*, 132. [\[CrossRef\]](#)
31. Tang, Z.; Li, C.; Kang, B.; Gao, G.; Li, C.; Zhang, Z. GEPIA: A Web Server for Cancer and Normal Gene Expression Profiling and Interactive Analyses. *Nucleic Acids Res.* **2017**, *45*, W98–W102. [\[CrossRef\]](#)
32. Uhlén, M.; Fagerberg, L.; Hallström, B.M.; Lindskog, C.; Oksvold, P.; Mardinoglu, A.; Sivertsson, Å.; Kampf, C.; Sjöstedt, E.; Asplund, A.; et al. Proteomics. Tissue-Based Map of the Human Proteome. *Science* **2015**, *347*, 1260419. [\[CrossRef\]](#)
33. Wang, L.-X.; Li, Y.; Chen, G.-Z. Network-Based Co-Expression Analysis for Exploring the Potential Diagnostic Biomarkers of Metastatic Melanoma. *PLoS ONE* **2018**, *13*, e0190447. [\[CrossRef\]](#)
34. Metri, R.; Mohan, A.; Nsengimana, J.; Pozniak, J.; Molina-Paris, C.; Newton-Bishop, J.; Bishop, D.; Chandra, N. Identification of a Gene Signature for Discriminating Metastatic from Primary Melanoma Using a Molecular Interaction Network Approach. *Sci. Rep.* **2017**, *7*, 17314. [\[CrossRef\]](#)
35. Huang, W.-C.; Jang, T.-H.; Tung, S.-L.; Yen, T.-C.; Chan, S.-H.; Wang, L.-H. A Novel MiR-365-3p/EHF/Keratin 16 Axis Promotes Oral Squamous Cell Carcinoma Metastasis, Cancer Stemness and Drug Resistance via Enhancing B5-Integrin/c-Met Signaling Pathway. *J. Exp. Clin. Cancer Res.* **2019**, *38*, 89. [\[CrossRef\]](#)
36. Elazezy, M.; Schwentesius, S.; Stegat, L.; Wikman, H.; Werner, S.; Mansour, W.Y.; Failla, A.V.; Peine, S.; Müller, V.; Thiery, J.P.; et al. Emerging Insights into Keratin 16 Expression during Metastatic Progression of Breast Cancer. *Cancers* **2021**, *13*, 3869. [\[CrossRef\]](#)
37. Ujiié, D.; Okayama, H.; Saito, K.; Ashizawa, M.; Thar Min, A.K.; Endo, E.; Kase, K.; Yamada, L.; Kikuchi, T.; Hanayama, H.; et al. KRT17 as a Prognostic Biomarker for Stage II Colorectal Cancer. *Carcinogenesis* **2020**, *41*, 591–599. [\[CrossRef\]](#)
38. Li, J.; Chen, Q.; Deng, Z.; Chen, X.; Liu, H.; Tao, Y.; Wang, X.; Lin, S.; Liu, N. KRT17 Confers Paclitaxel-Induced Resistance and Migration to Cervical Cancer Cells. *Life Sci.* **2019**, *224*, 255–262. [\[CrossRef\]](#)
39. Li, D.; Ni, X.-F.; Tang, H.; Zhang, J.; Zheng, C.; Lin, J.; Wang, C.; Sun, L.; Chen, B. KRT17 Functions as a Tumor Promoter and Regulates Proliferation, Migration and Invasion in Pancreatic Cancer via MTOR/S6k1 Pathway. *Cancer Manag. Res.* **2020**, *12*, 2087–2095. [\[CrossRef\]](#)
40. Wang, Z.; Yang, M.-Q.; Lei, L.; Fei, L.-R.; Zheng, Y.-W.; Huang, W.-J.; Li, Z.-H.; Liu, C.-C.; Xu, H.-T. Overexpression of KRT17 Promotes Proliferation and Invasion of Non-Small Cell Lung Cancer and Indicates Poor Prognosis. *Cancer Manag. Res.* **2019**, *11*, 7485–7497. [\[CrossRef\]](#)
41. Xiong, T.-F.; Pan, F.-Q.; Li, D. Expression and Clinical Significance of S100 Family Genes in Patients with Melanoma. *Melanoma Res.* **2019**, *29*, 23–29. [\[CrossRef\]](#)
42. Sakurai, M.; Miki, Y.; Takagi, K.; Suzuki, T.; Ishida, T.; Ohuchi, N.; Sasano, H. Interaction with Adipocyte Stromal Cells Induces Breast Cancer Malignancy via S100A7 Upregulation in Breast Cancer Microenvironment. *Breast Cancer Res.* **2017**, *19*, 70. [\[CrossRef\]](#)
43. Muoio, M.G.; Talia, M.; Lappano, R.; Sims, A.H.; Vella, V.; Cirillo, F.; Manzella, L.; Giuliano, M.; Maggiolini, M.; Belfiore, A.; et al. Activation of the S100A7/RAGE Pathway by IGF-1 Contributes to Angiogenesis in Breast Cancer. *Cancers* **2021**, *13*, 621. [\[CrossRef\]](#)
44. Tian, T.; Li, X.; Hua, Z.; Ma, J.; Wu, X.; Liu, Z.; Chen, H.; Cui, Z. S100A7 Promotes the Migration, Invasion and Metastasis of Human Cervical Cancer Cells through Epithelial-Mesenchymal Transition. *Oncotarget* **2017**, *8*, 24964–24977. [\[CrossRef\]](#)
45. Lin, M.; Xia, B.; Qin, L.; Chen, H.; Lou, G. S100A7 Regulates Ovarian Cancer Cell Metastasis and Chemoresistance Through MAPK Signaling and Is Targeted by MiR-330-5p. *DNA Cell Biol.* **2018**, *37*, 491–500. [\[CrossRef\]](#)
46. Hibino, T.; Sakaguchi, M.; Miyamoto, S.; Yamamoto, M.; Motoyama, A.; Hosoi, J.; Shimokata, T.; Ito, T.; Tsuboi, R.; Huh, N.-H. S100A9 Is a Novel Ligand of EMMPRIN That Promotes Melanoma Metastasis. *Cancer Res.* **2013**, *73*, 172–183. [\[CrossRef\]](#)
47. Hwang, S.-H.; Ahn, J.-H.; Lee, M. Upregulation of S100A9 Contributes to the Acquired Resistance to BRAF Inhibitors. *Genes Genom.* **2019**, *41*, 1273–1280. [\[CrossRef\]](#)
48. Jiang, Y.; Wang, Q.; Xu, Q.; Zhang, S.; Cao, L. Predictive Value of S100A9 for Lymph Node Metastasis in Cervical Cancer. *Zhong Nan Da Xue Xue Bao Yi Xue Ban* **2020**, *45*, 701–708. [\[CrossRef\]](#)
49. Lv, Z.; Li, W.; Wei, X. S100A9 Promotes Prostate Cancer Cell Invasion by Activating TLR4/NF-KB/Integrin B1/FAK Signaling. *OncoTargets Ther.* **2020**, *13*, 6443–6452. [\[CrossRef\]](#)
50. Zhou, C.; Shen, S.; Moran, R.; Deng, N.; Marbán, E.; Melmed, S. Pituitary Somatotroph Adenoma-Derived Exosomes: Characterization of Nonhormonal Actions. *J. Clin. Endocrinol. Metab.* **2022**, *107*, 379–397. [\[CrossRef\]](#)
51. Yang, X.; Liang, R.; Liu, C.; Liu, J.A.; Cheung, M.P.L.; Liu, X.; Man, O.Y.; Guan, X.-Y.; Lung, H.L.; Cheung, M. SOX9 Is a Dose-Dependent Metastatic Fate Determinant in Melanoma. *J. Exp. Clin. Cancer Res.* **2019**, *38*, 17. [\[CrossRef\]](#)

52. Cheng, P.F.; Shakhova, O.; Widmer, D.S.; Eichhoff, O.M.; Zingg, D.; Frommel, S.C.; Belloni, B.; Raaijmakers, M.I.; Goldinger, S.M.; Santoro, R.; et al. Methylation-Dependent SOX9 Expression Mediates Invasion in Human Melanoma Cells and Is a Negative Prognostic Factor in Advanced Melanoma. *Genome Biol.* **2015**, *16*, 42. [\[CrossRef\]](#) [\[PubMed\]](#)
53. Sun, T.; Liu, Z.; Zhang, R.; Ma, S.; Lin, T.; Li, Y.; Yang, S.; Zhang, W.; Wang, Y. Long Non-Coding RNA LEF1-AS1 Promotes Migration, Invasion and Metastasis of Colon Cancer Cells Through MiR-30-5p/SOX9 Axis. *Onco Targets Ther.* **2020**, *13*, 2957–2972. [\[CrossRef\]](#) [\[PubMed\]](#)
54. Zhou, T.; Wu, L.; Ma, N.; Tang, F.; Yu, Z.; Jiang, Z.; Li, Y.; Zong, Z.; Hu, K. SOX9-Activated FARSA-AS1 Predetermines Cell Growth, Stemness, and Metastasis in Colorectal Cancer through Upregulating FARSA and SOX9. *Cell Death Dis.* **2020**, *11*, 1071. [\[CrossRef\]](#) [\[PubMed\]](#)
55. Yasumoto, M.; Sakamoto, E.; Ogasawara, S.; Isobe, T.; Kizaki, J.; Sumi, A.; Kusano, H.; Akiba, J.; Torimura, T.; Akagi, Y.; et al. Muscle RAS Oncogene Homolog (MRAS) Recurrent Mutation in Borrmann Type IV Gastric Cancer. *Cancer Med.* **2017**, *6*, 235–244. [\[CrossRef\]](#)
56. Young, L.C.; Hartig, N.; Muñoz-Alegre, M.; Osés-Prieto, J.A.; Durdu, S.; Bender, S.; Vijayakumar, V.; Vietri Rudan, M.; Gewinner, C.; Henderson, S.; et al. An MRAS, SHOC2, and SCRIB Complex Coordinates ERK Pathway Activation with Polarity and Tumorigenic Growth. *Mol. Cell* **2013**, *52*, 679–692. [\[CrossRef\]](#)
57. Sun, Y.; Jia, X.; Hou, L.; Liu, X. Screening of Differently Expressed MiRNA and MRNA in Prostate Cancer by Integrated Analysis of Transcription Data. *Urology* **2016**, *94*, 313.e1–313.e6. [\[CrossRef\]](#)
58. Faruk, M.; Ibrahim, S.; Aminu, S.M.; Adamu, A.; Abdullahi, A.; Suleiman, A.M.; Rafindadi, A.H.; Mohammed, A.; Iliyasu, Y.; Idoko, J.; et al. Prognostic Significance of BIRC7/Livin, Bcl-2, P53, Annexin V, PD-L1, DARC, MSH2 and PMS2 in Colorectal Cancer Treated with FOLFOX Chemotherapy with or without Aspirin. *PLoS ONE* **2021**, *16*, e0245581. [\[CrossRef\]](#)
59. Yang, Y.; Sun, P.; Xu, W.; Xia, W. High BIRC7 Expression Might Be an Independent Prognostic Indicator of Poor Recurrence-Free Survival in Patients with Prostate Cancer. *Technol. Cancer Res. Treat.* **2018**, *17*, 1533033818809694. [\[CrossRef\]](#)
60. Liu, K.; Yu, Q.; Li, H.; Xie, C.; Wu, Y.; Ma, D.; Sheng, P.; Dai, W.; Jiang, H. BIRC7 Promotes Epithelial-Mesenchymal Transition and Metastasis in Papillary Thyroid Carcinoma through Restraining Autophagy. *Am. J. Cancer Res.* **2020**, *10*, 78–94.
61. Li, J.; Yang, Z.; Huang, S.; Li, D. BIRC7 and STC2 Expression Are Associated With Tumorigenesis and Poor Outcome in Extrahepatic Cholangiocarcinoma. *Technol. Cancer Res. Treat.* **2020**, *19*, 1533033820971676. [\[CrossRef\]](#)
62. Sun, K.; Liao, Q.; Chen, Z.; Chen, T.; Zhang, J. Expression of Livin and PlGF in Human Osteosarcoma Is Associated with Tumor Progression and Clinical Outcome. *Oncol. Lett.* **2018**, *16*, 4953–4960. [\[CrossRef\]](#)
63. Hsieh, C.-H.; Lin, Y.-J.; Wu, C.-P.; Lee, H.-T.; Shyu, W.-C.; Wang, C.-C. Livin Contributes to Tumor Hypoxia-Induced Resistance to Cytotoxic Therapies in Glioblastoma Multiforme. *Clin. Cancer Res.* **2015**, *21*, 460–470. [\[CrossRef\]](#)
64. Lazar, I.; Perlman, R.; Lotem, M.; Peretz, T.; Ben-Yehuda, D.; Kadouri, L. The Clinical Effect of the Inhibitor of Apoptosis Protein Livin in Melanoma. *Oncology* **2012**, *82*, 197–204. [\[CrossRef\]](#)
65. Yuan, B.; Ran, B.; Wang, S.; Liu, Z.; Zheng, Z.; Chen, H. SiRNA Directed against Livin Inhibits Tumor Growth and Induces Apoptosis in Human Glioma Cells. *J. Neurooncol.* **2012**, *107*, 81–87. [\[CrossRef\]](#)
66. Zhuang, L.; Shen, L.-D.; Li, K.; Yang, R.-X.; Zhang, Q.-Y.; Chen, Y.; Gao, C.-L.; Dong, C.; Bi, Q.; Tao, J.-N.; et al. Inhibition of Livin Expression Suppresses Cell Proliferation and Enhances Chemosensitivity to Cisplatin in Human Lung Adenocarcinoma Cells. *Mol. Med. Rep.* **2015**, *12*, 547–552. [\[CrossRef\]](#)
67. Liu, J.; Yang, Y.; Li, H.; Liu, Y.; Sun, Y.; Wu, J.; Xiong, Z.; Jin, T. IL1R2 Polymorphisms Are Associated with Increased Risk of Esophageal Cancer. *Curr. Mol. Med.* **2020**, *20*, 379–387. [\[CrossRef\]](#) [\[PubMed\]](#)
68. Zhang, L.; Qiang, J.; Yang, X.; Wang, D.; Rehman, A.U.; He, X.; Chen, W.; Sheng, D.; Zhou, L.; Jiang, Y.-Z.; et al. IL1R2 Blockade Suppresses Breast Tumorigenesis and Progression by Impairing USP15-Dependent BMI1 Stability. *Adv. Sci.* **2020**, *7*, 1901728. [\[CrossRef\]](#)
69. Torricelli, C.; Carron, J.; Carvalho, B.F.; Macedo, L.T.; Rinck-Junior, J.A.; Lima, C.S.P.; Lourenço, G.J. Influence of IL1B (Rs16944) and IL1R2 (Rs4141134) Polymorphisms on Aggressiveness and Prognosis of Cutaneous Melanoma. *Melanoma Res.* **2021**, *31*, 476–481. [\[CrossRef\]](#)
70. Yuan, M.; Wang, L.; Huang, H.; Li, Y.; Zheng, X.; Shao, Q.; Jiang, J. IL-1R2 Expression in Human Gastric Cancer and Its Clinical Significance. *Biosci. Rep.* **2021**, *41*, BSR20204425. [\[CrossRef\]](#)
71. Mar, A.-C.; Chu, C.-H.; Lee, H.-J.; Chien, C.-W.; Cheng, J.-J.; Yang, S.-H.; Jiang, J.-K.; Lee, T.-C. Interleukin-1 Receptor Type 2 Acts with c-Fos to Enhance the Expression of Interleukin-6 and Vascular Endothelial Growth Factor A in Colon Cancer Cells and Induce Angiogenesis. *J. Biol. Chem.* **2015**, *290*, 22212–22224. [\[CrossRef\]](#)
72. Ballerini, P.; Struski, S.; Cresson, C.; Prade, N.; Toujani, S.; Deswarte, C.; Dobbelstein, S.; Petit, A.; Lapillonne, H.; Gautier, E.-F.; et al. RET Fusion Genes Are Associated with Chronic Myelomonocytic Leukemia and Enhance Monocytic Differentiation. *Leukemia* **2012**, *26*, 2384–2389. [\[CrossRef\]](#) [\[PubMed\]](#)
73. Gao, F.; Zhang, Y.; Wang, S.; Liu, Y.; Zheng, L.; Yang, J.; Huang, W.; Ye, Y.; Luo, W.; Xiao, D. Hes1 Is Involved in the Self-Renewal and Tumorigenicity of Stem-like Cancer Cells in Colon Cancer. *Sci. Rep.* **2014**, *4*, 3963. [\[CrossRef\]](#)
74. Gao, F.; Huang, W.; Zhang, Y.; Tang, S.; Zheng, L.; Ma, F.; Wang, Y.; Tang, H.; Li, X. Hes1 Promotes Cell Proliferation and Migration by Activating Bmi-1 and PTEN/Akt/GSK3 β Pathway in Human Colon Cancer. *Oncotarget* **2015**, *6*, 38667–38680. [\[CrossRef\]](#) [\[PubMed\]](#)

75. Li, Y.; Zhang, Y.; Liu, X.; Wang, M.; Wang, P.; Yang, J.; Zhang, S. Lutein Inhibits Proliferation, Invasion and Migration of Hypoxic Breast Cancer Cells via Downregulation of HES1. *Int. J. Oncol.* **2018**, *52*, 2119–2129. [\[CrossRef\]](#)
76. Cenciarelli, C.; Marei, H.E.; Zonfrillo, M.; Casalbore, P.; Felsani, A.; Giannetti, S.; Trevisi, G.; Althani, A.; Mangiola, A. The Interference of Notch1 Target Hes1 Affects Cell Growth, Differentiation and Invasiveness of Glioblastoma Stem Cells through Modulation of Multiple Oncogenic Targets. *Oncotarget* **2017**, *8*, 17873–17886. [\[CrossRef\]](#)
77. Jiang, J.; Liu, X. Upregulated EBI3 Correlates with Poor Outcome and Tumor Progression in Breast Cancer. *Oncol. Res. Treat.* **2018**, *41*, 111–115. [\[CrossRef\]](#)
78. Hou, Y.-M.; Dong, J.; Liu, M.-Y.; Yu, S. Expression of Epstein-Barr Virus-Induced Gene 3 in Cervical Cancer: Association with Clinicopathological Parameters and Prognosis. *Oncol. Lett.* **2016**, *11*, 330–334. [\[CrossRef\]](#)
79. Yonekura, S. Epstein-Barr Virus-Induced Gene 3 as a Novel Biomarker in Metastatic Melanoma With Infiltrating CD8+ T Cells: A Study Based on The Cancer Genome Atlas (TCGA). *Anticancer Res.* **2022**, *42*, 511–517. [\[CrossRef\]](#)
80. Liu, Z.; Liu, J.-Q.; Shi, Y.; Zhu, X.; Liu, Z.; Li, M.-S.; Yu, J.; Wu, L.-C.; He, Y.; Zhang, G.; et al. Epstein-Barr Virus-Induced Gene 3-Deficiency Leads to Impaired Antitumor T-Cell Responses and Accelerated Tumor Growth. *Oncoimmunology* **2015**, *4*, e989137. [\[CrossRef\]](#)
81. Han, Y.; Li, X.; Yan, J.; Ma, C.; Wang, X.; Pan, H.; Zheng, X.; Zhang, Z.; Gao, B.; Ji, X.-Y. Bioinformatic Analysis Identifies Potential Key Genes in the Pathogenesis of Melanoma. *Front. Oncol.* **2020**, *10*, 581985. [\[CrossRef\]](#)
82. Leick, K.M.; Rodriguez, A.B.; Melssen, M.M.; Benamar, M.; Lindsay, R.S.; Eki, R.; Du, K.-P.; Parlak, M.; Abbas, T.; Engelhard, V.H.; et al. The Barrier Molecules Junction Plakoglobin, Filaggrin, and Dystonin Play Roles in Melanoma Growth and Angiogenesis. *Ann. Surg.* **2019**, *270*, 712–722. [\[CrossRef\]](#)
83. Wu, J.; Lu, Y.; Qin, A.; Qiao, Z.; Jiang, X. Overexpression of RAB34 Correlates with Poor Prognosis and Tumor Progression in Hepatocellular Carcinoma. *Oncol. Rep.* **2017**, *38*, 2967–2974. [\[CrossRef\]](#)
84. Sun, L.; Xu, X.; Chen, Y.; Zhou, Y.; Tan, R.; Qiu, H.; Jin, L.; Zhang, W.; Fan, R.; Hong, W.; et al. Rab34 Regulates Adhesion, Migration, and Invasion of Breast Cancer Cells. *Oncogene* **2018**, *37*, 3698–3714. [\[CrossRef\]](#)
85. Wang, H.; Gao, Y.; Chen, L.; Li, Y.; Jiang, C. RAB34 Was a Progression- and Prognosis-Associated Biomarker in Gliomas. *Tumour Biol.* **2015**, *36*, 1573–1578. [\[CrossRef\]](#)
86. Leucci, E.; Vendramin, R.; Spinazzi, M.; Laurette, P.; Fiers, M.; Wouters, J.; Radaelli, E.; Eyckerman, S.; Leonelli, C.; Vanderheyden, K.; et al. Melanoma Addiction to the Long Non-Coding RNA SAMMSON. *Nature* **2016**, *531*, 518–522. [\[CrossRef\]](#)
87. Han, S.; Yan, Y.; Ren, Y.; Hu, Y.; Wang, Y.; Chen, L.; Zhi, Z.; Zheng, Y.; Shao, Y.; Liu, J. LncRNA SAMMSON Mediates Adaptive Resistance to RAF Inhibition in BRAF-Mutant Melanoma Cells. *Cancer Res.* **2021**, *81*, 2918–2929. [\[CrossRef\]](#)
88. Somura, H.; Iizuka, N.; Tamesa, T.; Sakamoto, K.; Hamaguchi, T.; Tsunedomi, R.; Yamada-Okabe, H.; Sawamura, M.; Eramoto, M.; Miyamoto, T.; et al. A Three-Gene Predictor for Early Intrahepatic Recurrence of Hepatocellular Carcinoma after Curative Hepatectomy. *Oncol. Rep.* **2008**, *19*, 489–495. [\[CrossRef\]](#)
89. Berberich, A.; Bartels, F.; Tang, Z.; Knoll, M.; Pusch, S.; Hucke, N.; Kessler, T.; Dong, Z.; Wiestler, B.; Winkler, F.; et al. LAPTM5-CD40 Crosstalk in Glioblastoma Invasion and Temozolomide Resistance. *Front. Oncol.* **2020**, *10*, 747. [\[CrossRef\]](#)
90. Li, X.; Su, Y.; Zhang, J.; Zhu, Y.; Xu, Y.; Wu, G. LAPTM5 Plays a Key Role in the Diagnosis and Prognosis of Testicular Germ Cell Tumors. *Int. J. Genom.* **2021**, *2021*, 8816456. [\[CrossRef\]](#)
91. Yao, C.D.; Haensel, D.; Gaddam, S.; Patel, T.; Atwood, S.X.; Sarin, K.Y.; Whitson, R.J.; McKellar, S.; Shankar, G.; Aasi, S.; et al. AP-1 and TGF β Cooperativity Drives Non-Canonical Hedgehog Signaling in Resistant Basal Cell Carcinoma. *Nat. Commun.* **2020**, *11*, 5079. [\[CrossRef\]](#)
92. Barros-Silva, J.D.; Linn, D.E.; Steiner, I.; Guo, G.; Ali, A.; Pakula, H.; Ashton, G.; Peset, I.; Brown, M.; Clarke, N.W.; et al. Single-Cell Analysis Identifies LY6D as a Marker Linking Castration-Resistant Prostate Luminal Cells to Prostate Progenitors and Cancer. *Cell Rep.* **2018**, *25*, 3504–3518.e6. [\[CrossRef\]](#) [\[PubMed\]](#)
93. Wang, J.; Fan, J.; Gao, W.; Wu, Y.; Zhao, Q.; Chen, B.; Ding, Y.; Wen, S.; Nan, X.; Wang, B. LY6D as a Chemoresistance Marker Gene and Therapeutic Target for Laryngeal Squamous Cell Carcinoma. *Stem Cells Dev.* **2020**, *29*, 774–785. [\[CrossRef\]](#) [\[PubMed\]](#)
94. Mayama, A.; Takagi, K.; Suzuki, H.; Sato, A.; Onodera, Y.; Miki, Y.; Sakurai, M.; Watanabe, T.; Sakamoto, K.; Yoshida, R.; et al. OLFM4, LY6D and S100A7 as Potent Markers for Distant Metastasis in Estrogen Receptor-Positive Breast Carcinoma. *Cancer Sci.* **2018**, *109*, 3350–3359. [\[CrossRef\]](#) [\[PubMed\]](#)
95. Lu, Y.; Lemon, W.; Liu, P.-Y.; Yi, Y.; Morrison, C.; Yang, P.; Sun, Z.; Szoke, J.; Gerald, W.L.; Watson, M.; et al. A Gene Expression Signature Predicts Survival of Patients with Stage I Non-Small Cell Lung Cancer. *PLoS Med.* **2006**, *3*, e467. [\[CrossRef\]](#)
96. Kang, X.; Kong, F.; Huang, K.; Li, L.; Li, Z.; Wang, X.; Zhang, W.; Wu, X. LncRNA MIR210HG Promotes Proliferation and Invasion of Non-Small Cell Lung Cancer by Upregulating Methylation of CACNA2D2 Promoter via Binding to DNMT1. *Onco Targets Ther.* **2019**, *12*, 3779–3790. [\[CrossRef\]](#)
97. Warnier, M.; Roudbaraki, M.; Derouiche, S.; Delcourt, P.; Bokhobza, A.; Prevarskaya, N.; Mariot, P. CACNA2D2 Promotes Tumorigenesis by Stimulating Cell Proliferation and Angiogenesis. *Oncogene* **2015**, *34*, 5383–5394. [\[CrossRef\]](#)
98. Rossi, E.; Picozzi, P.; Bodega, B.; Lavazza, C.; Carlo-Stella, C.; Marozzi, A.; Ginelli, E. Forced Expression of RDH10 Gene Retards Growth of HepG2 Cells. *Cancer Biol. Ther.* **2007**, *6*, 238–244. [\[CrossRef\]](#)
99. Sun, E.; Liu, K.; Zhao, K.; Wang, L. Serine/Threonine Kinase 32C Is Overexpressed in Bladder Cancer and Contributes to Tumor Progression. *Cancer Biol. Ther.* **2019**, *20*, 307–320. [\[CrossRef\]](#)

100. Liu, Z.; Liu, X.; Cao, W.; Hua, Z.-C. Tumor-Specific Hypoxia-Induced Therapy of SPRY1/2 Displayed Differential Therapeutic Efficacy for Melanoma. *Am. J. Cancer Res.* **2015**, *5*, 792–801.
101. Ahn, J.-H.; Han, B.-I.; Lee, M. Induction of Resistance to BRAF Inhibitor Is Associated with the Inability of Spry2 to Inhibit BRAF-V600E Activity in BRAF Mutant Cells. *Biomol. Ther.* **2015**, *23*, 320–326. [\[CrossRef\]](#)
102. Fong, C.W.; Chua, M.-S.; McKie, A.B.; Ling, S.H.M.; Mason, V.; Li, R.; Yusoff, P.; Lo, T.L.; Leung, H.Y.; So, S.K.S.; et al. Sprouty 2, an Inhibitor of Mitogen-Activated Protein Kinase Signaling, Is down-Regulated in Hepatocellular Carcinoma. *Cancer Res.* **2006**, *66*, 2048–2058. [\[CrossRef\]](#)
103. Holderfield, M.; Deuker, M.M.; McCormick, F.; McMahon, M. Targeting RAF Kinases for Cancer Therapy: BRAF Mutated Melanoma and Beyond. *Nat. Rev. Cancer* **2014**, *14*, 455–467. [\[CrossRef\]](#)
104. Stecca, B.; Mas, C.; Clement, V.; Zbinden, M.; Correa, R.; Piguet, V.; Beermann, F.; Ruiz, I.; Altaba, A. Melanomas Require HEDGEHOG-GLI Signaling Regulated by Interactions between GLI1 and the RAS-MEK/AKT Pathways. *Proc. Natl. Acad. Sci. USA* **2007**, *104*, 5895–5900. [\[CrossRef\]](#)
105. Vlčková, K.; Réda, J.; Ondrušová, L.; Krayem, M.; Ghanem, G.; Vachtenheim, J. GLI Inhibitor GANT61 Kills Melanoma Cells and Acts in Synergy with Obatoclox. *Int. J. Oncol.* **2016**, *49*, 953–960. [\[CrossRef\]](#)
106. Liang, G.; Liu, M.; Wang, Q.; Shen, Y.; Mei, H.; Li, D.; Liu, W. Itraconazole Exerts Its Anti-Melanoma Effect by Suppressing Hedgehog, Wnt, and PI3K/MTOR Signaling Pathways. *Oncotarget* **2017**, *8*, 28510–28525. [\[CrossRef\]](#)
107. Pietrobono, S.; Gaudio, E.; Gagliardi, S.; Zitani, M.; Carrassa, L.; Migliorini, F.; Petricci, E.; Manetti, F.; Makukhin, N.; Bond, A.G.; et al. Targeting Non-Canonical Activation of GLI1 by the SOX2-BRD4 Transcriptional Complex Improves the Efficacy of HEDGEHOG Pathway Inhibition in Melanoma. *Oncogene* **2021**, *40*, 3799–3814. [\[CrossRef\]](#)
108. Chen, J.K.; Taipale, J.; Cooper, M.K.; Beachy, P.A. Inhibition of Hedgehog Signaling by Direct Binding of Cyclopamine to Smoothened. *Genes Dev.* **2002**, *16*, 2743–2748. [\[CrossRef\]](#)
109. Trnski, D.; Sabol, M.; Gojević, A.; Martinić, M.; Ozretić, P.; Musani, V.; Ramić, S.; Levanat, S. GSK3 β and Gli3 Play a Role in Activation of Hedgehog-Gli Pathway in Human Colon Cancer-Targeting GSK3 β Downregulates the Signaling Pathway and Reduces Cell Proliferation. *Biochim. Biophys. Acta* **2015**, *1852*, 2574–2584. [\[CrossRef\]](#)
110. Lauth, M.; Bergström, A.; Shimokawa, T.; Toftgård, R. Inhibition of GLI-Mediated Transcription and Tumor Cell Growth by Small-Molecule Antagonists. *Proc. Natl. Acad. Sci. USA* **2007**, *104*, 8455–8460. [\[CrossRef\]](#)
111. Han, J.; Sang, F.; Chang, J.; Hua, Y.; Shi, W.; Tang, L.; Liu, L. Arsenic Trioxide Inhibits Viability of Pancreatic Cancer Stem Cells in Culture and in a Xenograft Model via Binding to SHH-Gli. *Onco Targets Ther.* **2013**, *6*, 1129–1138. [\[CrossRef\]](#)
112. Mazumdar, T.; Devecchio, J.; Agyeman, A.; Shi, T.; Houghton, J.A. The GLI Genes as the Molecular Switch in Disrupting Hedgehog Signaling in Colon Cancer. *Oncotarget* **2011**, *2*, 638–645. [\[CrossRef\]](#)
113. Wickström, M.; Dyberg, C.; Shimokawa, T.; Milosevic, J.; Baryawno, N.; Fuskevåg, O.M.; Larsson, R.; Kogner, P.; Zaphiropoulos, P.G.; Johnsen, J.I. Targeting the Hedgehog Signal Transduction Pathway at the Level of GLI Inhibits Neuroblastoma Cell Growth in Vitro and in Vivo. *Int. J. Cancer* **2013**, *132*, 1516–1524. [\[CrossRef\]](#)
114. Miyazaki, Y.; Matsubara, S.; Ding, Q.; Tsukasa, K.; Yoshimitsu, M.; Kosai, K.; Takao, S. Efficient Elimination of Pancreatic Cancer Stem Cells by Hedgehog/GLI Inhibitor GANT61 in Combination with MTOR Inhibition. *Mol. Cancer* **2016**, *15*, 49. [\[CrossRef\]](#)
115. Santini, R.; Vinci, M.C.; Pandolfi, S.; Penachioni, J.Y.; Montagnani, V.; Olivito, B.; Gattai, R.; Pimpinelli, N.; Gerlini, G.; Borgognoni, L.; et al. HEDGEHOG-GLI Signaling Drives Self-Renewal and Tumorigenicity of Human Melanoma-Initiating Cells. *Stem Cells* **2012**, *30*, 1808–1818. [\[CrossRef\]](#)
116. Peer, E.; Tesanovic, S.; Aberger, F. Next-Generation Hedgehog/GLI Pathway Inhibitors for Cancer Therapy. *Cancers* **2019**, *11*, 538. [\[CrossRef\]](#) [\[PubMed\]](#)
117. Bakshi, A.; Chaudhary, S.C.; Rana, M.; Elmets, C.A.; Athar, M. Basal Cell Carcinoma Pathogenesis and Therapy Involving Hedgehog Signaling and Beyond. *Mol. Carcinog.* **2017**, *56*, 2543–2557. [\[CrossRef\]](#)
118. Wessler, S.; Krisch, L.M.; Elmer, D.P.; Aberger, F. From Inflammation to Gastric Cancer—The Importance of Hedgehog/GLI Signaling in Helicobacter Pylori-Induced Chronic Inflammatory and Neoplastic Diseases. *Cell Commun. Signal.* **2017**, *15*, 15. [\[CrossRef\]](#)
119. Akyala, A.I.; Peppelenbosch, M.P. Gastric Cancer and Hedgehog Signaling Pathway: Emerging New Paradigms. *Genes Cancer* **2018**, *9*, 1–10. [\[CrossRef\]](#)
120. Tsavachidou, D.; Coleman, M.L.; Athanasiadis, G.; Li, S.; Licht, J.D.; Olson, M.F.; Weber, B.L. SPRY2 Is an Inhibitor of the Ras/Extracellular Signal-Regulated Kinase Pathway in Melanocytes and Melanoma Cells with Wild-Type BRAF but Not with the V599E Mutant. *Cancer Res.* **2004**, *64*, 5556–5559. [\[CrossRef\]](#)
121. Chen, L.; Wang, G.; Luo, Y.; Wang, Y.; Xie, C.; Jiang, W.; Xiao, Y.; Qian, G.; Wang, X. Downregulation of LAPTM5 Suppresses Cell Proliferation and Viability Inducing Cell Cycle Arrest at G0/G1 Phase of Bladder Cancer Cells. *Int. J. Oncol.* **2017**, *50*, 263–271. [\[CrossRef\]](#)